APPLICATION OF SPACE-TIME TRELLIS CODES FOR IMAGE TRANSMISSION OVER WIRELESS CHANNELS

by

HESHAM MUHAMMAD IBRAHIM AL-SALMAN

A Thesis Presented to the
DEANSHIP OF GRADUATE STUDIES

In Partial Fulfillment of the Requirements
for the Degree

MASTER OF SCIENCE

in

ELECTRICAL ENGINEERING

KING FAHD UNIVERSITY OF PETROLEUM & MINERALS

DHAHRAN, SAUDI ARABIA

JUNE 2003

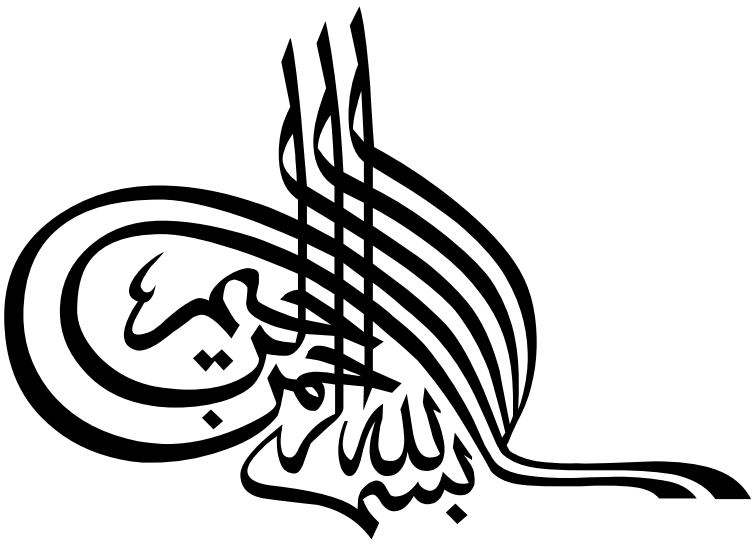
بسم الله الرحمن الرحيم

Dedicated to

My Parents

and

My Wife

Acknowledgment

In the name of Allah, the Most Gracious and the Most Merciful

All praise and glory goes to Almighty Allah (Subhanahu Wa Ta'ala) who gave me the courage and patience to carry out this work. Peace and blessings of Allah be upon His last Prophet Muhammad (Salla-Allah-o-Alaihi-Wa-Sallam) and all his Sahaba (Radhia-Allah-o-'Anhum) who devoted their lives towards the prosperity and spread of Islam.

Acknowledgment is due to King Fahd University of Petroleum and Minerals for providing support for this work.

My deep appreciation and gratitude goes to my thesis advisor Dr. Saud A. al-Semari for his constant endeavor, guidance and the numerous moments of attention he devoted throughout the course of this research work. His valuable suggestions made this work interesting and knowledgeable for me.

I extend my deepest gratitude to my thesis committee members Dr. Mahmoud

Dawoud and Dr. Maan Kousa for their encouragement, cooperation and for their valuable time that spent reviewing and correcting this work.

Acknowledgment is due to my fellow and friend Salam Adil Zummo, who provided me with many important resources and was very helpful and cooperative at all times. I also thank my fellow and friend Sami Abdul-Hadi Al-Anazi with whom I had informative discussions that helped me at various stages of this work.

Special thanks are due to colleagues and my friends for their encouragement, motivation and pivotal support. A few of them are Abdul-Malik Muhammad Al-Saeed, Badr Hamad Al-Dohan, Wail Abdul-Hakim Mousa, Omar Ghazi Al-Attas, Muhannad Abdullah Al-Turki and many others, all of whom I will not be able to name here. They were as good as friends and collegues can be.

And last but not the least, I would like to thank my parents; from the core of my heart. Their prayers and encouragement have always helped me take the right steps in life. May Allah reward them with the highest degrees in Jannah. A special thank is due to my dear wife who stood with me all the way. She was, and still is, the faithful and patient companion. Words are not enough to fulfill the thanks due to my whole family, but to whom I say may Allah reward you gracefully.

TABLE OF CONTENTS

List of Tables

List of Figures

THESIS ABSTRACT

NAME: HESHAM MUHAMMAD IBRAHIM AL-SALMAN

TITLE: APPLICATION OF SPACE-TIME TRELLIS CODES FOR IMAGE TRANSMISSION OVER WIRELESS CHANNELS

MAJOR: ELECTRICAL ENGINEERING

DATE OF DEGREE: JUNE, 2003

Since their introduction in 1998, the applications of space-time trellis codes have been, and still are, increasing rapidly. In this thesis, unequal error protecting ST trellis codes are designed then used to transmit images over a rapid fading channel. The idea is to use ST trellis codes that provide strong error protection to one of its multiple input bits and send the important part of the image through that bit. This requires modifying the existing performance measurement techniques such that they show the weight of error protection on each input bit. This is done using a modified transfer function and new upper bounds for each individual input bit. To find the desired codes, two approaches are used: design and exhaustive search. Both approaches are used to find several QPSK and 8PSK codes that provide strong error protection properties to the most significant bit. To complete the application, the JPEG image processing technique is modified to separate the important from the less important bits. Finally, test images are simulated using the new codes in addition to several codes from the literature for comparison.

خلاصة الرسالة

الاسم : **هشام بن محمد بن إبراهيم السلمان**

العنوان : **تطبيق الترميزات الفراغية الوقتية الشبكية لإرسال الصور عبر القنوات اللاسلكية**

التخصص: **هندسة كهربائية**

التاريخ : **ربيع الآخر 1424 هـ - يونيو 2003 م**

منذ تقديمها في عام 1998م وتطبيقات الترميزات الفراغية الوقتية في ازدياد مستمر. في هذه الرسالة يتم تصميم ترميزات فراغية وقتية شبكية بحماية غير متساوية واستخدامها لإرسال صور عبر قنوات سريعة التغير. الفكرة تكمن في استخدام ترميزات توفر حماية عالية ضد الأخطاء لواحد من البتات المتعددة الداخلة إلى المرمّز، ومن ثمّ إرسال الجزء الأكثر أهمية من الصورة خلال ذلك البت. حتى يتم التصميم يجب أن تعدل الوسائل الحالية المستخدمة في تقييم الترميزات الفراغية الوقتية الشبكية بحيث تظهر كمية الحماية ضد الأخطاء التي توفرها لكل بت على حدة. هذا التعديل يتم باستخدام كثيرة حدود ناقلة معدلة يُشتق منها حد أعلى لكل بت عل حدة. ولإيجاد الترميزات المطلوبة يتم استخدام وسيلتين هما البحث الكامل والتصميم. كلا الوسيلتين تستخدمان لإيجاد ترميزات عديدة بإشارات رُباعية وثمانية توفر حماية قوية للبت الأهم. ولإتمام التطبيق يجب تعديل الوسائل المتبعة في معالجة الصور بحيث يتم عزل البتات المهمة عن غيرها. وأخيراً حتى تتم تجربة الترميزات والطريقة الجديدة تستخدم صورة يحاكى ارسالها عبر قناة لاسلكية سريعة التغير باستخدام الترميزات الجديدة وأيضاً ترميزات أخرى للمقارنة.

CHAPTER 1

INTRODUCTION

1.1 INTRODUCTION

Multimedia applications in wireless devices (such as mobile phones) are growing more than ever. Applications like high quality audio and video streams are very appealing add-on's in today's mobile devices. Unfortunately, video transmission over band-limited wireless channels has always been a challenge. Problems ranging from low video quality to high bandwidth demand crippled adapting video transmission in mobile devices. The recent development in channel coding theory represented in space-time (ST) [1] codes opens wide doors for development in all high data-rate wireless communication systems. This new technology promises to solve some of the long-known problems with wireless channels.

Space-time codes rely on the idea of combining multiple transmit antennas with trellis-coded modulation. This resulted in a coding technique that provides both high transmission rate and strong error correction capabilities. More important is its capability of overcoming fading and inter-symbol-interference (ISI) that occur in wireless channels.

Using equal error protecting space-time trellis code that cannot give priority to the important information bits of the image might not give the best results. On the other hand, using unequal error protecting (UEP) ST trellis codes that provide strong error protection to the most significant input bit would enhance wireless image transmission quality. In other words, ST trellis codes that provide UEP to its multiple input bits are used to give the high importance part of the image more error protection and the less importance part is given less error protection.

This chapter begins with a brief description of fading channels and trellis codes as a laying foundation. Following that a typical space-time system is described. Then the performance criterion is analyzed and simulation of various ST systems is shown. A survey of recent research in the area follows. The chapter ends with stating the structure of this thesis and the contributions to the field.

1.2 Fading Channels

In addition to the *additive white Gaussian noise* (AWGN) model, the *fading channel* model is used to describe wireless channels.

Because of the time-variant nature of the channel, its response changes within a communication session. Depending on the rate of change, it is considered to be either *slow fading* (SF) or *fast fading* (FF) channel. In FF environments, the channel changes its gain at a larger rate than the symbol transmission rate, so that one symbol exhibits different attenuation gains. In SF environments, the channel gain changes in rate slower than the symbol rate. SF channels can be further classified into *quasi-static* and *rapid fading* channels. In quasi-static fading channels, the fade samples are assumed to be constant for the period of one frame (consisting of l_f codewords) and independent from one frame to the other. On the other hand, the fade samples in rapid fading channels change independently from one symbol to the other within the frame. The rapidity of the channel variations depends mainly on the speed of movement of the mobile handset. As it increases, the channel changes faster and hence the fade samples become less correlated in time.

Fading channels are statistically modeled using different probabilistic methods. Referring to [3], the distribution of the samples of a fading channel is generally modeled by a Rayleigh distribution. Therefore, the probability density function (pdf) of the channel fade amplitude samples ($|a|$) is:

$$f_a(|a|) = \frac{|a|}{\sigma^2} \exp\left(\frac{-|a|^2}{2\sigma^2}\right), \qquad a > 0 \tag{1.1}$$

Where $2\sigma^2$ is the average power of the fading samples, and the phase is uniformly

distributed on the period $[0, 2\pi]$. When a dominant line-of-sight (direct) path exists at the receiver, the pdf of the channel fade samples is Rician distributed.

To reduce the effect of multipath fading channels, several mitigation techniques are used. Equalization is used to cancel the ISI at the receiver resulting from the multipath phenomenon. It is simply a filter that performs the inverse effect of the channel. In order to know the effect of the channel on the transmitted signal, a training sequence known to the receiver is transmitted. This sequence is used to train the equalizer for the underlying channel so that it can cancel out the channel effects when the data is transmitted. There are various kinds of equalizers: the *linear equalizer* and the *decision feedback equalizer*. When *channel state information* (CSI) is known at the receiver, *maximum likelihood sequence estimation* provides better performance [3].

When the fade coefficients' values happen to be much smaller than 1, the received signal can be affected easily by the noise. To reduce the probability of having the channel at deep fades, the receiver can utilize diversity to get different versions of the transmitted signal. This can be done using either *receiver diversity* or *transmit diversity* [3].

Space diversity at the receiver is commonly widely used. It is implemented by having more than one antenna at the receiver in order to receive uncorrelated versions of the transmitted signal. It is necessary for the received versions at the receiver to be uncorrelated in order to maximize the probability of not having

them all at deep fades. Hence, receive antennas should be separated by a minimum distance that depends on the wavelength of the transmitted carrier. A satisfactory minimum separating distance is 10 times the radio wavelength [4]. Systems with space diversity at the receiver perform better than systems without diversity with the advantage of no bandwidth penalty. In such systems, a combining algorithm should be used at the receiver to combine signals received over different branches. Some of the known combining methods are the *equal-gain combining*, *maximal-ratio combining* (MRC) and *selection combining*. They vary in terms of performance and implementation complexity [3]. On the other hand, diversity can be provided from the transmitter side. This is done in two ways: *temporal diversity* and *antenna diversity*. In temporal diversity, the transmitter is responsible for providing the receiver by uncorrelated versions of the transmitted signal. This is done by transmitting the same signal more than one time resulting in bandwidth penalty and more transmission power. With antenna diversity, the same signal is transmitted at the same time and frequency over multiple transmit antennas. This is proved to perform better than systems using space diversity at the receiver [5]. Sending the same signal more than one time can be viewed as a repetition code. A more sophisticated approach is to use error correction codes in conjunction with interleaving at the transmitter and send the resulting signals using one antenna. This provides the receiver with replicas of the original signal in the form of redundancy. Trellis codes can be used to provide the required time diversity from the

transmitter side.

In frequency diversity, the same signal is transmitted in more than one frequency-division multiplexed (FDM) channels. The same concept can be applied in time domain. In time diversity, the same signal is transmitted over more than one interleaved time-division multiplexed (TDM) channels. Interleaving is required in order to provide time diversity and convert slow fading channels into independent fading ones, so that the received signals undergo independent fades.

1.3 TRELLIS CODED MODULATION

Trellis coded modulation (or simply trellis codes) is a combination of a convolutional code and a bandwidth-efficient signaling technique. The main idea behind developing trellis codes is to provide error detection/correction coding without sacrificing the transmission symbol rate. In other words, trellis coding avoids bandwidth expansion by integrating a coding technique (e.g. convolutional) with an expanded bandwidth-efficient signal set and utilize the redundancy resulting from such expansion.

Figure 1.1 shows a general trellis encoder. In it, k input bits are encoded by a $(k/k+1)$ trellis encoder. The $k+1$ bits are mapped onto a point from a $2^{(k+l)}$-ary signal set, such that the *minimum Euclidean distance* between channel-signal sequences is maximized. Inside the trellis encoder is a $(\widetilde{k}/\widetilde{k}+1)$ convolutional encoder where $\widetilde{k} \leq k$. In the case of $\widetilde{k} < k$ there are $\widetilde{k}-k$ uncoded bits resulting in

parallel transitions when departing from each state in the encoder. This generally reduces the Euclidean and Hamming distances between mapped symbols at these transitions.

In general, using trellis codes increases the constellation size of the output signal which reduces the Euclidean distance between symbols [6]. Ungerbeock proposed the *set partitioning method* to solve this problem [6]. He partitioned the resulting signal constellation into non-overlapping sets of symbols so that the Euclidean distance between symbols in the same set is larger than that of the original constellation. Ungeboeck introduced design rules to maximize the Euclidian distance [6].

Like convolutional codes, trellis codes are described by a trellis path. Therefore, the most popular decoding method of trellis is the Viterbi algorithm. For AWGN channels, the pairwise error probability of trellis codes is [6]:

$$P(\mathbf{s}_l, \hat{\mathbf{s}}_l) = \frac{1}{2}\,\mathrm{erfc}\left(\sqrt{\frac{d_E^2(\mathbf{s}_l, \hat{\mathbf{s}}_l)}{4\mathrm{N}_0}}\right) \tag{1.2}$$

Where $\mathbf{s}_l$ and $\hat{\mathbf{s}}_l$ are the correct and erroneous sequences of length l, respectively, i.e: $\mathbf{s}_l = (s_1, s_2, \ldots, s_l)$ and $\hat{\mathbf{s}}_l = (\hat{s}_1, \hat{s}_2, \ldots, \hat{s}_l)$. The factor $d_E^2(\mathbf{s}_l, \hat{\mathbf{s}}_l)$ is the free squared Euclidean distance between sequences $\mathbf{s}_l$ and $\hat{\mathbf{s}}_l$. For AWGN channels, the free squared Euclidean distance is the limiting factor of the performance of the trellis code. As the number of encoder's states is increased, the free squared Euclidean distance between two possible error events increases. There is an upper limit for

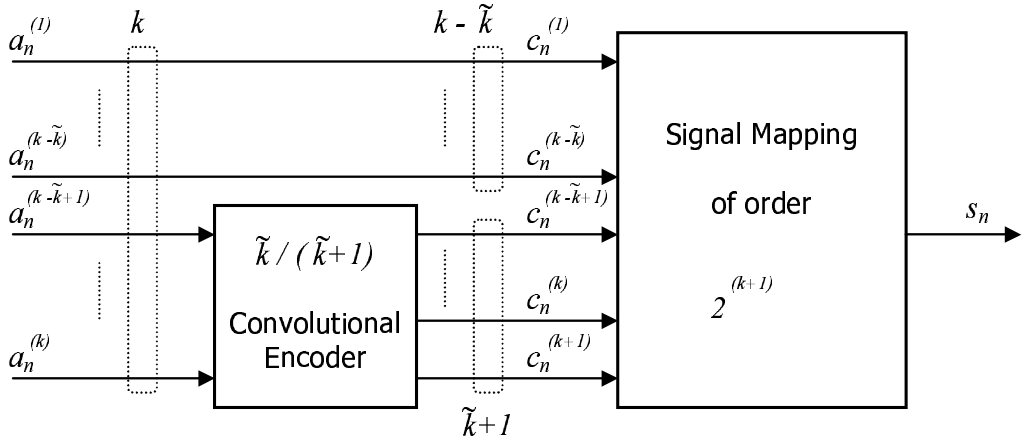

Figure 1.1: General block diagram of a trellis encoder

the number of states for which the free distance increases [6]. This limit depends on the number of branches leaving each state and the encoder's constraint length. Also, as the constellation size increases, set partitioning becomes more difficult and the required free squared Euclidean distance decreases. For AWGN channels, the optimal set partitioning is the one proposed by Ungerboeck [6].

In fading channels, the primary design parameters for good trellis codes are the *minimum time diversity* (MTD) of the code (or *effective length*) L and the *minimum squared product distance* (MSPD) $d_P^2(l_{\hat{\nu}})$ [6]. Defining $l_{\hat{\nu}}$ as the length of the error event $\hat{\nu}$ makes the minimum time diversity $L = \min(l_{\hat{\nu}})$. MTD is the minimum number of different symbols between all possible error events and the correct path. It is a symbol-wise Hamming distance, which represents the time diversity of the code. The MTD of the trellis code (L) is upper bounded by a value that depends on the number of states in the encoder as [6]:

$$L \leq \lfloor v/\widetilde{k} \rfloor + 1 \tag{1.3}$$

Where v is the number of memory elements of the encoder and $\widetilde{k}$ is the number of input bits to the convolutional encoder. The MSPD distance is the product of differences between each symbol in the shortest error event and that in the correct path.

The performance of trellis codes over Rayleigh and Rician fading channels was evaluated in [6]. It is shown that significant improvement can be achieved by

interleaving the outputs of the encoder, which randomizes the error distribution by destroying the memory of the channel. For Rayleigh fading channels, the pairwise error probability is upper bounded by (for ideal CSI):

$$\begin{aligned} \mathrm{P}(\mathbf{s}_l, \hat{\mathbf{s}}_l) &\leq \prod_{i \in \hat{\nu}} \left[\frac{|s_i - \hat{s}_i|^2}{4N_0} \right]^{-1} \\ &\leq \left[\left(\frac{1}{4N_0} \right)^{l_{\hat{\nu}}} d_p^2(l_{\hat{\nu}}) \right]^{-1} \end{aligned} \tag{1.4}$$

Where s_i and $\hat{s}_i$ are the i^{th} symbols in the correct sequence and the error event, respectively. The symbol $\hat{\nu}$ denotes the set of all i's for which $s_i \neq \hat{s}_i$.

In general, a trellis code designed to be optimal for AWGN channels may not be optimal for fading channels. Equation (1.4) shows that the code's MTD and MSPD are the main performance criteria. The design criterion for fading channels is to maximize L and d_p^2. Maximizing L is equivalent to increasing the diversity offered by the coded system.

1.4 Space-Time Codes

Space-time codes can be described as a combination of transmitter diversity and trellis encoding. They were first introduced in their present form by Tarokh *et al* in [1]. Nevertheless, the idea of combining trellis and time diversity was introduced in *multiple trellis coded modulation* (MTCM) by Divsalar and Simon in 1986 [7]. Space-transmitter diversity dates back to 1978 [1]. A special case of ST that is

called delay diversity was first introduced by Wittneben in 1993 [8].

1.4.1 Encoder/Decoder of ST Systems

A typical ST encoder is shown in Figure 1.2, where a convolutional encoder takes k input bits and encode them to $n \times \tilde{n}$ coded bits. These bits are then divided into n sets each consisting of $\tilde{n}$ bits. Every $\tilde{n}$ bits set is then mapped onto a point from a $2^{\tilde{n}}$-ary signal set. Finally, the resulting n symbols are modulated and transmitted at the same instance of time and at the same frequency. The decoder consists of m receive antennas sending the received signals to m demodulators then to a maximal-ratio combiner and a Viterbi decoder. Adjacent antennas at the transmitter and receiver are assumed to be separated by a distance that assures the independence of fading events. The following example will illustrate a typical ST encoder system.

Take a system consisting of a $(4, 2)$ convolutional encoder and 2 QPSK modulators each attached to an antenna. The convolutional encoder takes 2 bits input and gives 2 output bits to the first QPSK modulator and 2 output bits to the second QPSK modulator. The first transmission antennas transmits its signal at the same time instant and at the same frequency as the second antenna. Because the modulation scheme is QPSK, the output signal of each antenna will be one of 4 symbols (0, 1, 2 or 3). Figure 1.3 shows a 4-state QPSK ST with 2 bit/s/Hz encoder and decoder system from [1]. As seen from the trellis diagram (see Fig-

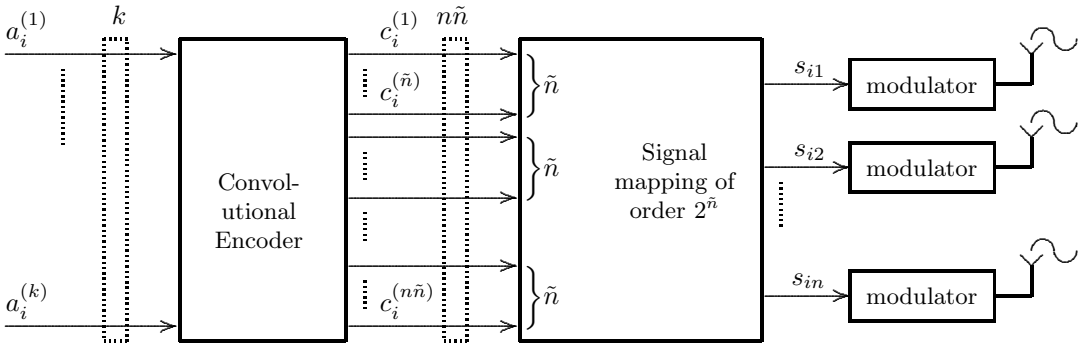

Figure 1.2: General block diagram of a space-time trellis encoder

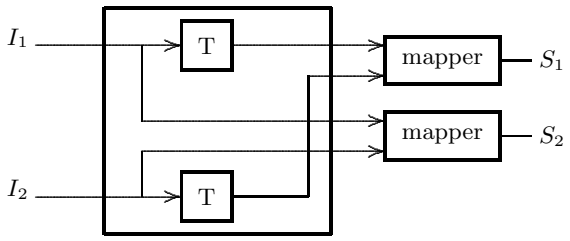

Figure 1.3: 4-State QPSK space-time encoder from [1]

ure 1.4(b)), this system has 4 states and 4 branches out of each state. There are 2 output symbols labeling each branch corresponding to the 2 transmission antennas. The outgoing branches are ordered such that the first branch corresponds to the input 00, the second branch corresponds to the input 01 and so on. If as an example the input sequence (10) (01) (11) is to be transmitted using this encoder, the output of the two antennas (1^{st} antenna, 2^{nd} antenna) would be (assuming that the initial state being 00) (1, 2) (3, 1) (0, 3). The first antenna is transmitting its symbols at the same time instant and frequency as the second antenna. This code can be viewed as a delay diversity system. In other words, the symbol transmitted over the first antenna at one time instant is the same symbol transmitted over the second antenna in the previous time slot. Hence, symbols transmitted over the second antenna will be transmitted over the first antenna with a delay of one symbol duration, which dictates the delay diversity system.

The received signal r_t^j at the j^{th} antenna at time t is a noisy superposition of all transmitted symbols over all transmit antennas and is given by:

$$r_t^j = \sum_{i=1}^{n} \alpha_{ij,t} c_t^i + \eta_t^j \tag{1.5}$$

where η_t^i is an AWGN modeled as independent samples of a zero-mean complex Gaussian random process with variance $N_0/2$ per dimension. The coefficient $\alpha_{ij,t}$ is the path gain from the i^{th} transmit antenna to the j^{th} receive antenna at time t and c_t^i is the transmitted symbol from the i^{th} transmit antenna at time t.

At the receiver side, the Viterbi decoder computes a branch metric defined by the following:

$$\sum_{j=1}^{m} |r_t^j - \sum_{i=1}^{n} \alpha_{ij,t}\, c_t^i|^2 \tag{1.6}$$

1.4.2 Performance Criteria of ST Systems

In [1] performance criteria for ST codes are derived for the cases of rapid and quasi-static fading channels.

The performance of ST codes over quasi-static channels is briefly presented in the following. Consider a sequence of codewords $\mathbf{C}_l$ that has been transmitted over l time intervals and was erroneously decoded as the sequence $\hat{\mathbf{C}}_l$ where:

$$\mathbf{C}_l = c_1^1 c_1^2 \ldots c_1^n\, c_2^1 c_2^2 \ldots c_2^n c_l^1\, c_l^2 \ldots c_l^n$$

$$\hat{\mathbf{C}}_l = \hat{c}_1^1 \hat{c}_1^2 \ldots \hat{c}_1^n\, \hat{c}_2^1 \hat{c}_2^2 \ldots \hat{c}_2^n\, \hat{c}_l^1 \hat{c}_l^2 \ldots \hat{c}_l^n$$

Here, l is the length of the sequence in time and n is the number of transmit antennas, resulting in a total of n codewords or $n \times l$ symbols in the codeword sequence $\mathbf{C}_l$. The pairwise error probability of deciding $\mathbf{C}_l$ in favor of $\hat{\mathbf{C}}_l$ using maximum likelihood decoding is upper bounded by the Chernoff bound [1] as:

$$P(\mathbf{C}_l, \hat{\mathbf{C}}_l | \alpha_{ij},\ i = 1, 2, \ldots, n,\ j = 1, 2, \ldots, m) \leq \exp\left(\frac{-d_E^2(\mathbf{C}_l, \hat{\mathbf{C}}_l)}{4N_0}\right) \tag{1.7}$$

where

$$d_E^2(\mathbf{C}_l, \hat{\mathbf{C}}_l) = \sum_{t=1}^{l} \sum_{j=1}^{m} E_s \left| \sum_{i=1}^{n} \alpha_{ij} (c_t^i - \hat{c}_t^i) \right|^2 \tag{1.8}$$

The quantity in the inner summation represents Euclidean distance between the i^{th} symbol in the correct sequence and that in the decoded one. The quantity inside the middle summation is the metric computed for a transition between two states in the encoder. As mentioned for quasi-static channels, the fade samples are assumed to be constant for one frame period of length l and hence the time subscript is omitted. The total expression $d_E^2(\mathbf{C}_l, \hat{\mathbf{C}}_l)$ is the accumulated path metric between the two sequences.

This expression can be evaluated for *independent fade coefficients* to the following [1]:

$$\mathrm{P}(\mathbf{C}_l, \hat{\mathbf{C}}_l | \beta_{ij}) \leq \left[\left(\prod_{i=1}^{r} \lambda_i \right)^{1/r} \frac{E_s}{4N_0} \right]^{-rm} \tag{1.9}$$

Where r is the number of nonzero eigenvalues of the matrix A, where A is an $n \times n$ matrix with:

$$\mathrm{A_{pq}}(c_l, \hat{c}_l) = \sum_{t=1}^{l} (c_t^p - \hat{c}_t^p) \cdot (c_t^q - \hat{c}_t^q) \tag{1.10}$$

Note that the remaining $(n - r)$ eigenvalues do not contribute to the above inequality. The diversity advantage of the ST code is defined to be the gain in the SNR over the system without diversity, and the coding gain is the gain in SNR over uncoded systems when operating at the same diversity advantage. From Equation (1.9), the diversity advantage is rm, and the coding gain is $(\prod_{i=1}^{r} \lambda_i)^{1/r}$.

According to these parameters, the code design must satisfy some conditions that maximize both the diversity and coding advantages. These are summarized by the rank and determinant criteria.

The rank criterion tells that the matrix A must be full rank (i.e: its rank equals n) in order to achieve maximum diversity order nm. If a diversity order of rm is the target, then the rank of that matrix must be at least equal to r. The determinant criterion says that a coding gain is maximized if the product of all nonzero eigenvalues λ_i's maximized. This is equivalent to maximizing the minimum determinant of A for all pairs of distinct possible codewords.

The same criteria with some changes are applied when the fading samples of the transmit branches are correlated. Performance of ST codes over quasi-static fading channels with correlated branches is worse than that over quasi-static channels with independent branches due to the dependency between the fading coefficients from one transmit branch to another one.

For the rapid fading case, in which the fading process changes from one sampling time to the other, the rank criterion is called the distance criterion that maximizes the diversity advantage. Moreover, the determinant criterion is called product criterion and it should be maximized in order to achieve the maximum coding advantage [1].

In [1] performance criteria developed above are used to set rules for the design of ST codes over quasi-static fading channels. Some codes satisfying these rules

are designed and simulated in [1] for quasi-static channels. Some of those results are reproduced here in Figure 1.5 for 4, 8 and 16-state QPSK case. The code trellis diagrams are shown in Figure 1.4(b). The code performance can generally be improved by increasing the number of receive antennas. This is shown via simulation in Figure 1.6.

The codes presented in [1] are not the only codes satisfying the rank and determinant criterion. Moreover, they are not optimum neither in quasi-static nor in rapid fading channels. Many codes found recently outperform codes in [1] for the same complexity. More advanced code construction and search criteria presented in [9], [10], [11], [12], [13] and many more (see the following section) lead researchers to find better performing codes. Some of these codes are shown in Figure 1.4(c) for the 4-state QPSK case. Their performance for quasi-static and rapid fading channels is shown in Figure 1.7 and Figure 1.8 respectively.

1.4.3 Recent Research

Improvements on the design rules of [1] were introduced by Grimm and Fitz in [14] and produced better performing codes. The search for optimum codes lead Bäro *et al* [9] to find better performing codes through systematic search in all possible codes using the same criteria in [1]. Blum in [15] introduced an analytical tool for finding optimum codes and reached the same 4-state code found in [9] to be optimum. Furthermore, he found a more powerful code for the 8-state case than

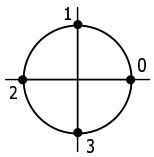

(a)

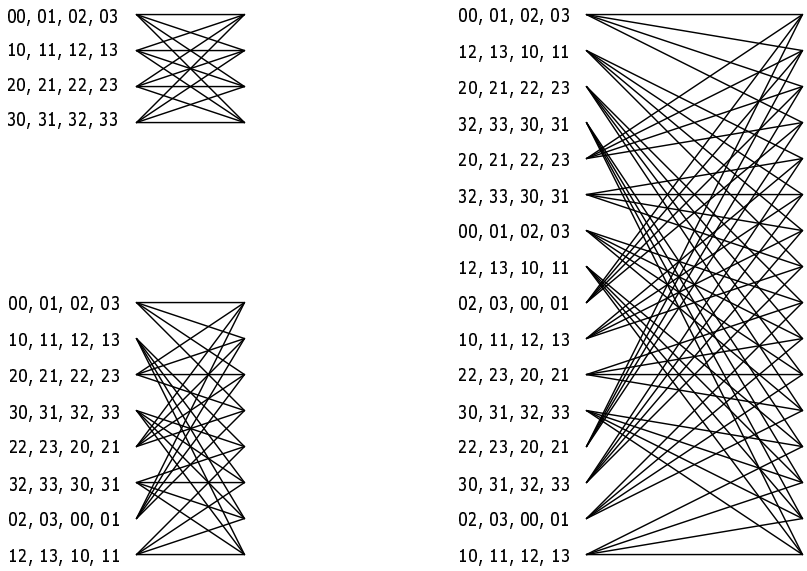

(b)

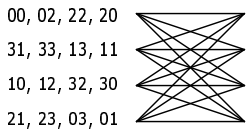

(c)

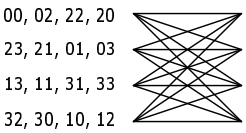

(d)

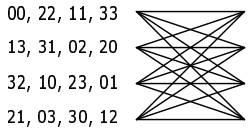

(e)

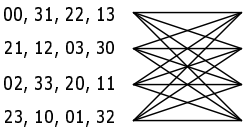

(f)

Figure 1.4: (a) QPSK signal constellations, (b) 4, 8 and 16-state codes from [1], (c) B-B-H [9], (d) Da Silva [13], (e) Z-S [10], (f) F-V-Y [12]

.

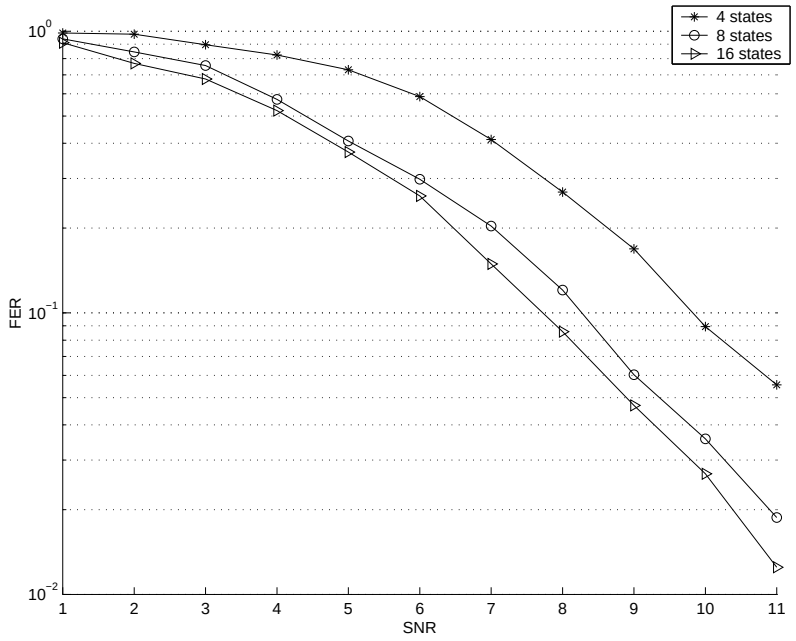

Figure 1.5: Performance of 4, 8 and 16-state codes of [1]

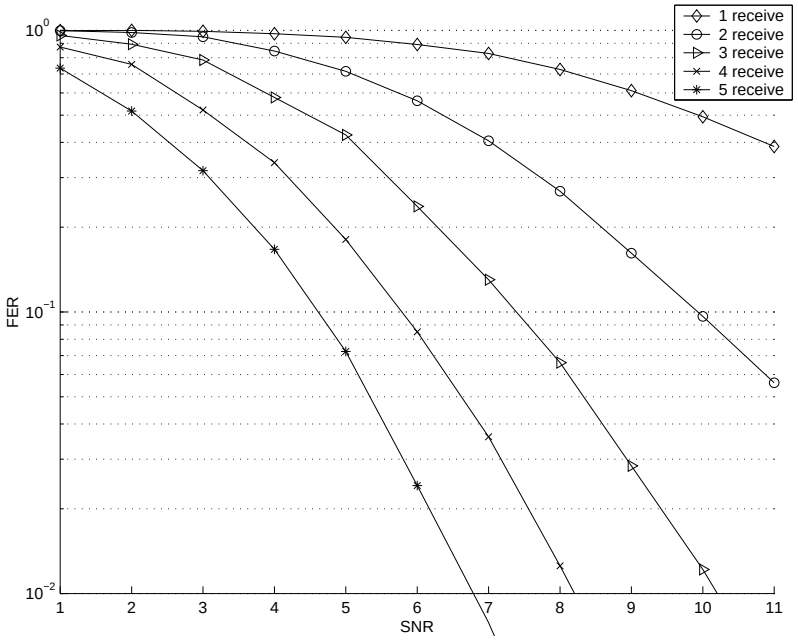

Figure 1.6: Performance of 1, 2, 3, 4 and 5 receive antennas for the 4-state code of [1]

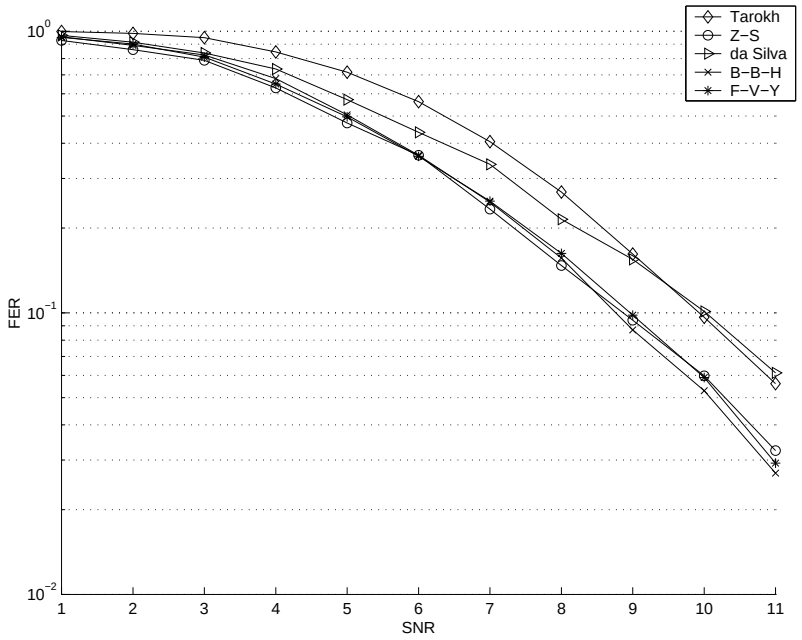

Figure 1.7: Performance of the 4-state codes from Figure 1.4 in quasi-static fading channel

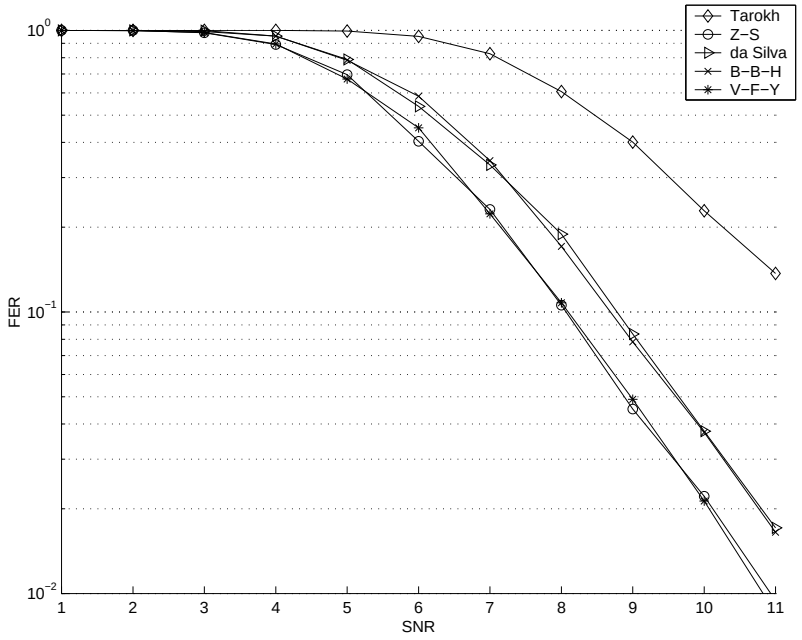

Figure 1.8: Performance of the 4-state codes from Figure 1.4 in rapid fading channel

the one found in [9]. Further results and more optimum codes are found in [11]. This search of better codes is found in a number of papers [13], [16], and [10] all of which introduce codes that are better performing than the first introduced ones. Hammons and El Gamal [17] introduced new conditions on generator matrices instead of on every code word pair to ensure full space diversity for the case of BPSK and multiple transmit antennas. The results in [17] were extended by Fitz *et al* in [18] to include all 2^{2k} QAM modulation for any positive integer k. This rank criterion simplifies the check of full space diversity. Siwamogsatham and Fitz in [19] noticed that the codes designed in [5] degrade drastically in Rayleigh fading channels with certain space-time correlations. So they proposed a coding scheme that achieve robust performance in correlated Rayleigh fading channels.

Enhancements to space-time codes are introduced in many papers. QPSK Space-time turbo codes for quasi-static to fast fading channels are investigated in [20]. In this paper the codes were designed based on the rank criterion of [18] and are tested on different channel and code parameters conditions to check their robustness and performance. In [12] new codes were introduced to improve the performance over fast fading channels. Lin and Blum in [21] introduced *serial concatenation* to improve the performance of the known codes. They also designed ST codes employing MTCM in [22] and showed that these codes can have larger coding gains compared to conventional ST-trellis codes. For channels with non-negligible ISI Fitz *et al* in [23] proposed design rules to achieve maximum level

diversity. A joint decoding and equalization algorithm with decision feedback method is presented in [24] as a solution for ISI.

Performance analysis for ST codes is found in a number of papers. Fitz *et al* in [23] introduced an asymptotically tight bound on the pair-wise error probability. Zummo and Al-Semari in [25] introduced a tightening constant for the pairwise error of ST codes over rapid fading channels. Their new bound is shown to be tighter than the older one by almost 2 dBs and is very tight for the simulation results. Aktas and Fitz in [26] and [27] expanded the distance spectrum for quasi-static channels, which depend on the rank and determinant criteria. The authors proposed a distance spectrum computation method that uses a reduced error state diagram. They demonstrated their method by finding the distance spectrum for several codes.

An applications of ST codes in *continuous phase modulation* (CPM) by Zhang and Fitz is found in [28]. Here, a design criterion of ST codes in CPM systems is presented. An example code was designed and simulated with and without an *interleaver*. Another application of ST codes for *direct sequence code division multiple access* (DS-CDMA) is presented in [29]. Zhang and and Blum in [30] applied a space-time turbo code for use in a CDMA system.

1.5 THESIS CONTRIBUTION AND ORGANIZATION

One main objective of this research is to enhance image transmission over rapid fading channels using unequal error protecting ST trellis codes. Therefore, as a starter, an ST trellis encoder/decoder system have been simulated and several codes from the literature were used to reproduce the results and test the system over quasi-regular and rapid fading channels. All the work in the literature never considered ST trellis codes that provide different error protection levels depending on the position of the input bit into the encoder. Nevertheless, there are other approaches to implement unequal error protection. These approaches include using more power, higher rates and/or more complex codes to deliver the added protection to the most important information bits. One important aspect of the work in this thesis is that there is no price to pay using codes that *naturally* offer unequal error protection to input bits, because there is no change in the complexity, power or rate of the encoder/decoder system. Such codes that provide strong protection to the most significant bit are useful in applications where information bits are not equally important. One such application is image transmission since the image's low frequency components are far more important than the high frequency ones.

In order to find ST trellis codes that provide very strong error protection on the most significant bit, two approaches are introduced in this thesis. The first is an *exhaustive search* approach which is performed in two steps. First, all possible codes of a certain modulation scheme and a certain number of states are generated

assuming a linear encoder. Then, all generated codes are passed through a series of tests to find the best ones satisfying the *search criteria*. To speed up this lengthy process, the programming is done in C language. The second approach is a *design approach*, in which a new 7-step design technique is introduced. Although there are good design approaches in the literature, but none of them consider the weight of error protection on different input bits. This new design technique considers the task of addressing input bits individually in terms of error protection weight. Hence, it is capable of handcrafting codes that provide unequal error protection to the input bits depending on their position into the encoder. Both approaches are used to find several QPSK and 8PSK codes providing strong error protection properties to the most significant bit. The new codes are simulated over a rapid fading channel and their performance is compared to existing codes in the literature.

The search and design approaches cannot be built using the classical tools in the literature since they do not show the weight of error protection on different input bits. The classical transfer function does not consider addressing input bits individually. Therefore, a modified version of it that shows the weight of error protection on every input bit is derived. From the *modified transfer function* the current upper-bounds for the code in general are extended to derive upper-bounds for every input bit to the encoder individually. Expanding the transfer to find the distance spectrum of general trellis codes is a complicated task. Yet, it is necessary

for transfer function enumeration, and hence, upper-bounds calculations. Distance spectrum calculation can be simplified if the code shows a certain amount of symmetry. One such symmetry is quasi-regularity which was originally introduced to trellis codes. In this thesis, the definition of quasi-regularity is extended to include ST trellis codes.

Before completing the application of image transmission, the image must be processed first. The processing is done such that it follows, as much as possible, the popular JPEG standard. The image is transformed then quantized. The last step in JPEG image processing requires the use of variable length coding for source coding. This leads to catastrophic errors at channels with low signal-to-noise ratios. Hence, a modified approach that uses fixed length zonal coding is used here. This approach reduces the number of bits to represent coefficients (similarly to variable length coding) using the fact that most of the image power is in the DC coefficient and the first AC ones. The digitized image is divided into more than one bit stream according to importance. This bit division is what makes use of the added protection to the MSB. A test image is processed and sent over a rapid fading channel using several codes from the literature and the new codes found using the search and design approaches.

To sum up the contributions of this thesis in a few points:

- A modified version of the transfer function that shows the weight of error protection on every input bit is derived.

- From the modified transfer function, new upper bounds for every individual input bits are derived.
- The definition of quasi-regularity is extended to ST trellis codes to simplify distance spectrum calculation.
- General guidelines on UEP code design and search are devised.
- A C program is written to implement the exhaustive search approach which includes code generation and code search using a specific search criteria.
- A new 7-steps design technique that considers the task of addressing input bits individually is introduced.
- Both approaches are used to find 4, 8 and 16-state QPSK and 8-state 8PSK codes providing strong error protection properties to the most significant bit.
- A modified approach that divides the image into more than one bit stream according to importance is developed and used.
- Image transmission quality over a wireless channel is improved for relatively low SNR using the new codes.
- Additional improvement is introduced using code concatenation.

This thesis is organized as follows. This chapter is an introduction to space-time trellis codes and fading channels. It includes a literature survey of the recent

research in the field. The chapter ends with the thesis contribution and organization. Chapter 2 provides the tools necessary to the codes design and search methods. It begins by reviewing current upper-bounds of pairwise error probability and bit error probability (BEP) for ST trellis codes over rapid fading channels. Then, the current transfer function is introduced then modified to reflect the weight of protection on different input bits. Following that new BEP upper bounds for individual input bits are derived from the modified transfer function. The upper-bound calculations are done using the the modified distance spectrum. Then, the definition of quasi-regularity for trellis codes is given and extended to ST trellis codes to simplify the distance spectrum expansion. Finally, several examples of the new upper-bounds, distance spectrum and quasi-regularity are found in the chapter.

Chapter 3 contains the two approaches of search and design of UEP ST trellis codes. It begins with the code search criteria and methodology. A method of code generation followed by a search criteria is proposed. Then a 7-step new code design method is introduced. Both approaches are applied to 4, 8, and 16-state QPSK and 8-state 8PSK codes. The new codes are simulated and compared to codes from the literature to evaluate their performance.

The application of image transmission is in Chapter 4. The chapter begins by an introduction to image processing, which covers transform coding followed by quantization. Then, the binary bits are divided into most significant bits and least

significant bits. The new codes, in addition to several codes from the literature are used to send the binary bits over a rapid fading channel. Several comparison images and plots are provided to show the improvement of using the new codes compared to other codes in the literature.

Finally, the main conclusions, findings, and extension of this work are summarized in Chapter 5.

CHAPTER 2

PERFORMANCE EVALUATION OF UEP ST TRELLIS CODES

2.1 INTRODUCTION

After presenting the performance evaluation of ST trellis codes over quasi-static fading channels in Chapter 1, the performance of ST trellis codes using pairwise error, error event and bit error probabilities is described in this chapter for rapid fading channels. As will be explained later on in this chapter, bit error probability (BEP) evaluation requires enumeration of the transfer function (TF) using the distance spectrum (DS) calculation. Therefore, the transfer function and distance spectrum of ST trellis codes are introduced. In order to simplify TF and DS calculations, quasi-regularity (a code symmetry property first introduced to trellis

codes) should be extended to ST trellis codes.

The classical TF and DS do not show the weight of different input bits, which is a goal of this thesis. Therefore, a modified version of the TF that reflects the error protection weight of different input bits, is derived. From this modified TF, BEP upper-bounds for each input bit are also derived. These modified performance merits are used in the next chapter to set the guidelines for the design of UEP ST trellis codes. The chapter also contains several examples of upper bounds for individual input bits, distance spectrum tables, quasi-regular and non-quasi-regular codes and their performance.

2.2 Performance Evaluation

Take the ST trellis system described in Chapter 1 and shown in Figure 1.2, where a convolutional encoder takes k input bits and encodes them to $n \times \tilde{n}$ coded bits. These bits are divided into n sets, each consisting of $\tilde{n}$ bits. Every $\tilde{n}$ bits set is then mapped onto a point from a $2^{\tilde{n}}$-ary signal set. Finally, the resulting n symbols are modulated and transmitted at the same time instance and at the same frequency. The decoder consists of m receive antennas passing the received signals to m demodulators then to a maximal-ratio combiner and a Viterbi decoder.

Recall that the received signal r_t^j at the j^{th} antenna at time t is a noisy super-

position of all transmitted symbols over all transmit antennas and is given by:

$$r_t^j = \sum_{i=1}^{n} \alpha_{i,j}(t) c_t^i \sqrt{E_s} + \eta_t^j \tag{2.1}$$

where η_t^i is an AWGN modeled as independent samples of a zero-mean complex Gaussian random process with variance $N_0/2$ per dimension. The coefficient $\alpha_{i,j}(t)$ is the path gain from the i^{th} transmit antenna to the j^{th} receive antenna and c_t^i is the transmitted symbol from the i^{th} transmit antenna at time t. For the performance evaluation in this section a rapid fading channel with independent fade coefficients (i.e. fade coefficients change independently, with time, from one fade coefficient to another) is going to be considered.

At the receiver side, the Viterbi decoder computes a branch metric defined by the following:

$$\sum_{j=1}^{m} |r_t^j - \sum_{i=1}^{n} \alpha_{i,j}(t)\, c_t^i|^2 \tag{2.2}$$

2.2.1 Pairwise Error and Error Event Probabilities

Take two codeword sequences $\mathbf{C}_l$ and $\hat{\mathbf{C}}_l$ where

$$\mathbf{C}_l = c_1^1 c_1^2 \ldots c_1^n \; c_2^1 c_2^2 \ldots c_2^n \; c_l^1 c_l^2 \ldots c_l^n$$

$$\hat{\mathbf{C}}_l = \hat{c}_1^1 \hat{c}_1^2 \ldots \hat{c}_1^n \; \hat{c}_2^1 \hat{c}_2^2 \ldots \hat{c}_2^n \; \hat{c}_l^1 \hat{c}_l^2 \ldots \hat{c}_l^n$$

From the expanded trellis diagram of the code, two paths of finite length form an error event if they start from the same state, merge in the same state, and do not simultaneously occupy the same state in between. Mathematically, an error event of length l is defined by two codeword sequences $\mathbf{C}_l$ and $\hat{\mathbf{C}}_l$ such that

$$\begin{aligned} C_i &= \hat{C}_i \qquad \text{for} \quad i = 0, l \\ C_i &\neq \hat{C}_i \qquad \text{for} \quad i = 1, 2, \ldots, l-1 \end{aligned}$$

Take $\mathbf{C}_l$ as the correct transmitted codeword sequence and $\hat{\mathbf{C}}_l$ is the one erroneously chosen by the maximum likelihood decoder. The probability of choosing $\hat{\mathbf{C}}_l$ over $\mathbf{C}_l$ is the *pairwise error probability* (PEP) and is denoted by $P(\hat{\mathbf{C}}_l, \mathbf{C}_l)$. For a rapid fading channel, assuming maximum likelihood decoding, PEP is upper bounded by [1]:

$$P(\mathbf{C}_l, \hat{\mathbf{C}}_l) \leq \prod_{t \in \hat{\nu}} D \tag{2.3}$$

where

$$D = \left(1 + \sum_{i=1}^{n} |c_t^i - \hat{c}_t^i|^2 \frac{E_s}{4N_0}\right)^{-m} \tag{2.4}$$

and $\hat{\nu}$ denotes the set of time instances such that $|c_t^i - \hat{c}_t^i|^2 \neq 0$.

It can be seen from (2.3) that in order to *minimize* the pairwise symbol error probability of space-time trellis codes over rapid fading channels, two main criteria must be *maximized* [1]:

- *The Distance Criterion:* The *symbol differences* between codewords $\mathbf{c}_t$ and

$\hat{\mathbf{c}}_t$ should be maximized. When two codes have the same distance properties, the next criterion distinguish them.

- *The Product Criterion:* The *minimum* of the following product should also be maximized:

$$\prod_{t\in\hat{\nu}}\sum_{i=1}^{n}|c_t^i-\hat{c}_t^i|^2$$

For codes having the same minimum symbol-differences and minimum product-distance properties, the performance depends on higher *product distances* (not just the minimum) and the *multiplicities* of those paths (i.e. the number of paths with the same distance properties).

The probability of an error event starting at time time 0 , given that the decoder has estimated the correct transmitter state at that time, is called *error event probability* (EEP) or P_e and can be upper bounded by [6]:

$$P_e \leq \frac{1}{2}\sum_{l=1}^{\infty}\sum_{\mathbf{C}_l}\sum_{\mathbf{C}_l\neq\hat{\mathbf{C}}_l}P(\mathbf{C}_l)P(\mathbf{C}_l,\hat{\mathbf{C}}_l) \tag{2.5}$$

where $P(\mathbf{C}_l)$ is the *a priori* probability of transmitting $\mathbf{C}_l$.

Let $\mathbf{A}_l=(\mathbf{a}_0,\mathbf{a}_1,\ldots,\mathbf{a}_l)$ and $\hat{\mathbf{A}}_l=(\hat{\mathbf{a}}_0,\hat{\mathbf{a}}_1,\ldots,\hat{\mathbf{a}}_l)$ be two *binary* label sequences corresponding to $\mathbf{C}_l$ and $\hat{\mathbf{C}}_l$, respectively. Considering a one-to-one mapping function μ between the output codewords and their labels, the upper bound can be expressed in terms of labels rather than codeword signals. The two binary labels $\mathbf{A}_l$ and $\hat{\mathbf{A}}_l$ can be related by introducing a sequence of binary error vectors

$\mathbf{E}_l = (\mathbf{e}_0, \mathbf{e}_1, \ldots, \mathbf{e}_l)$ as:

$$\hat{\mathbf{a}}_i = \mathbf{a}_i \oplus \mathbf{e}_i, \qquad i = 0, 1, \ldots, l \tag{2.6}$$

where $\oplus$ denotes modulo-2 (binary) addition. By replacing $\mathbf{C}_l$ and $\hat{\mathbf{C}}_l$ by their labels in (2.5) and using (2.6), the upper bound of error event probability can be written as:

$$\begin{aligned} P_e &\leq \frac{1}{2}\sum_{l=1}^{\infty}\sum_{\mathbf{A}_l}\sum_{\mathbf{A}_l \neq \hat{\mathbf{A}}_l} P(\mathbf{A}_l)P(\mathbf{A}_l, \hat{\mathbf{A}}_l) \\ &= \frac{1}{2}\sum_{l=1}^{\infty}\sum_{\mathbf{A}_l}\sum_{\mathbf{E}_l \neq 0} P(\mathbf{A}_l)P(\mathbf{A}_l, \mathbf{A}_l \oplus \mathbf{E}_l) \end{aligned} \tag{2.7}$$

Substituting (2.3) into (2.5) yields:

$$P_e \leq \frac{1}{2}\sum_{l=1}^{\infty}\sum_{\mathbf{A}_l}\sum_{\mathbf{E}_l \neq 0} P(\mathbf{A}_l)\prod_{t \in \hat{\nu}} D \tag{2.8}$$

2.3 Quasi-Regularity of ST Trellis Codes

It is desirable to calculate the distance spectrum as a method to enumerate the transfer function and evaluate bit error probability upper-bound (see Section 2.4). In order to calculate the distance spectrum of a general trellis code, one must calculate the product distances between all possible paths between any two states. Biglieri [31] described a general method that uses an expanded set of N^2 states.

Needless to say that this method is very difficult for codes with relatively large number of states. Many researchers afterward explored symmetries of certain trellis codes to reduce the number of states needed to calculate the distance spectrum (see for example [32], [33], [34], [35], and [36]). In all these papers, researchers proved that the code symmetries enabled to calculate the product distance between all possible paths and the all-zero path only without loss of generality [37].

An important note here is to distinguish between the merits of performance measurement for ST trellis over quasi-static and rapid fading channels. For quasi-static channels the merits are the rank and determinant criteria, while for rapid fading channels the merits are the distance and product criteria (see Section 2.2.1 for rapid fading channels and [1] for both). This leads to a difference in the complexity reduction technique. The work presented here is meant for rapid fading channels only. For other work concerning quasi-static channels and different approach in complexity reduction, the reader is referred to the work of Aktas and Fitz [26] and [27].

One such symmetry is quasi-regularity introduced by Rouanne and Costello in [32]. In this approach, the Euclidian distances between output symbols are found as polynomials of error vector labels. If a code is quasi-regular, then its distance spectrum can be calculated assuming the all-zero path being transmitted.

Let σ and $\hat{\sigma}$ be two states in the code trellis (the notations here follow those of Benedetto *et al* [37]), and $\mathbf{e} = e_0, e_1, \ldots, e_k$ be a vector representing a binary

$(k+1)$-tuple, called the *error vector*. The distance polynomial $P_{\sigma,\hat{\sigma},\mathbf{e}}(D)$ is defined as:

$$P_{\sigma,\hat{\sigma},\mathbf{e}}(D) = \sum_{\mathbf{a}|\sigma} p(\mathbf{a}|\sigma) D^{d^2[\mu(\mathbf{a}),\, \mu(\mathbf{a}\oplus\mathbf{e})]} \tag{2.9}$$

where $p(\mathbf{a}|\sigma)$ is the probability that the binary label vector $\mathbf{a}$ labels a transition originating from the state σ, and $d^2[\mu(\mathbf{a}), \mu(\mathbf{a}\oplus\mathbf{e})]$ is the squared Euclidean distance between signals $\mu(\mathbf{a})$ (originating from σ) and signals $s(\mathbf{a}\oplus\mathbf{e})$ (originating from $\hat{\sigma}$), which are labeled by two binary $(k+1)$-tuple which differ by $\mathbf{e}$. The summation in (2.9) is extended over all vectors $\mathbf{a}$ labeling transitions originating from σ.

Definition 1 *A trellis scheme is said to be quasi-regular if [32]:*

1. *its encoder is linear,*

2. *for all* $\mathbf{e}$ *and for all pairs of states* $(\sigma_i, \hat{\sigma}_i)$ *and* $(\sigma_j, \hat{\sigma}_j)$

$$P_{\sigma_i,\hat{\sigma}_i,\mathbf{e}}(D) = P_{\sigma_j,\hat{\sigma}_j,\mathbf{e}}(D) \tag{2.10}$$

To verify Condition (2), each pair of states must be considered and the polynomials for each admissible error vector $\mathbf{e}$ must be constructed.

In the case of ST trellis codes, unlike conventional trellis codes, they have more than one output symbol. Therefore, the labels for the error vectors and for the output symbols are used n-times (where n is the number of output antennas). To demonstrate this feature consider the code of Figure 2.1. For the output symbols

(2 3), the binary labels are (10 11), where the (10) corresponds to the output symbol of the first antenna (2) and (11) corresponds to the output symbol of the second antenna (3).

Example 1 *To demonstrate quasi-regularity of ST trellis codes, take the code of Example 2 shown in Figure 2.1.*

This code can be realized as a linear encoder followed by a mapper as can be seen from Figure 2.3. The next step is to verify the second condition of quasi-regularity definition.

Consider the two states σ_0 and σ_1 and the error vector $\mathbf{e} = \{0000\}$. Because the binary labels of state σ_0 (0000,0001,0010,0011) are different from those originating from state σ_1 (0100,0101,0110,0111), the polynomial $P_{0,1,0000}$ is not defined and one can proceed to the next error vector $\mathbf{e} = \{0100\}$. In this case the polynomial is defined because the set of labels of the signals leaving σ_1 is obtained by adding the error vector $\mathbf{e} = \{0100\}$ to the set of labels leaving state σ_0. Therefore the polynomial $P_{0,1,0100}$ is given by:

$$\begin{aligned} P_{0,1,0100}(D) &= p(0000|0)D^{\mathrm{d}^2[\mu(0000),\mu(0100)]} + \ldots \\ &\quad + p(0011|0)D^{\mathrm{d}^2[\mu(0011),\mu(0111)]} \\ &= D^{\delta_0^2} \end{aligned}$$

Where Euclidean distances δ_0 and δ_1 are as given in Figure 2.2 and Table 2.1.

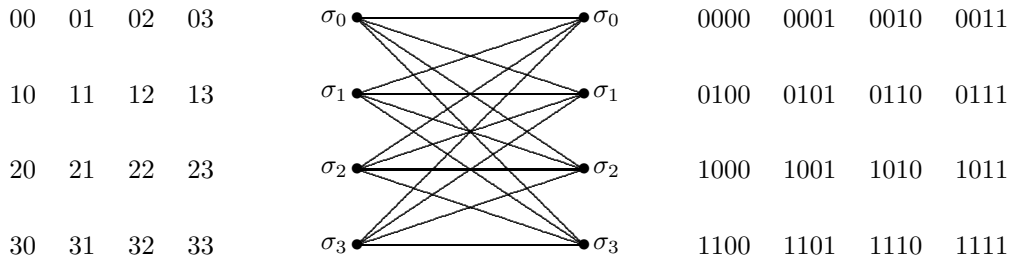

Figure 2.1: Trellis diagram of Code of Example 1 and the binary labeling vectors

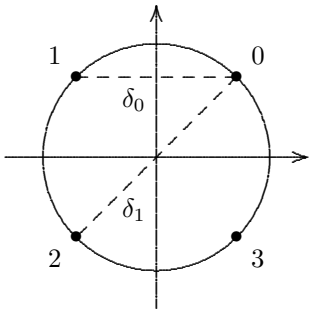

Figure 2.2: Constellation points of a QPSK system

TABLE 2.1: EUCLIDEAN DISTANCES FOR ERROR VECTORS

		error vector			
symbol	label	00	01	10	11
0	00	0	δ_0^2	δ_1^2	δ_0^2
1	01	0	δ_0^2	δ_1^2	δ_0^2
2	10	0	δ_0^2	δ_1^2	δ_0^2
3	11	0	δ_0^2	δ_1^2	δ_0^2

Then the search for other pairs of states with the error vector $\mathbf{e} = \{0100\}$ between its labels is continued. It is found that $P_{2,3,0100}$ is defined, and:

$$\begin{aligned} P_{2,3,0100}(D) &= p(0000|0)D^{\mathrm{d}^2[\mu(0000),\mu(0100)]} + \ldots \\ &\quad + p(0011|0)D^{\mathrm{d}^2[\mu(0011),\mu(0111)]} \\ &= D^{\delta_0^2} \end{aligned}$$

It can be seen that there are no other pairs of states have the error vector $\mathbf{e} = \{0100\}$ is defined. Doing the previous procedure for all possible error vectors that are defined and all pairs of states, the following distance polynomials are obtained:

$$\begin{aligned} P_{0000} &= 1, & P_{0100} &= D^{\delta_0^2}, \\ P_{1000} &= D^{\delta_1^2}, & P_{1100} &= D^{\delta_0^2}, \\ P_{0001} &= D^{\delta_0^2}, & P_{0101} &= D^{2\delta_0^2}, \\ P_{1001} &= D^{\delta_0^2+\delta_1^2}, & P_{1101} &= D^{2\delta_0^2}, \\ P_{0010} &= D^{\delta_0^2}, & P_{0110} &= D^{\delta_0^2+\delta_1^2}, \\ P_{1010} &= D^{2\delta_1^2}, & P_{1110} &= D^{\delta_0^2+\delta_1^2}, \\ P_{0011} &= D^{\delta_0^2}, & P_{0111} &= D^{2\delta_0^2}, \\ P_{1011} &= D^{\delta_0^2+\delta_1^2}, & P_{1111} &= D^{2\delta_0^2} \end{aligned}$$

One can check that for all $\mathbf{e}$ and for all of states $(\sigma_i, \hat{\sigma}_i)$ and $(\sigma_j, \hat{\sigma}_j)$:

$$P_{\sigma_i,\hat{\sigma}_i,\mathbf{e}}(D) = P_{\sigma_j,\hat{\sigma}_j,\mathbf{e}}(D)$$

Thus, proving its quasi-regularity.

2.4 TRANSFER FUNCTION

The *Transfer function* of an *error-state diagram* with N states is a function that characterizes the code by enumerating all possible error sequences. The error-state diagram is derived from the code state diagram by labeling its branches with error weight profile. It can be represented as [6]:

$$T(D) = \frac{1}{2^k} \sum_{l=1}^{\infty} \sum_{\mathbf{E}_l \neq 0} \prod_{t \in \hat{\nu}} D \tag{2.11}$$

It can be seen from (2.8) and (2.11) that the error event probability can be evaluated by using the transfer function method if the term $\sum_{\mathbf{A}_l} P(\mathbf{A}_l)$ in (2.8) can be expressed in a product form. This can be done for general cases by introducing an error-state diagram whose branches have $N \times N$ matrix labels [7]. For the case of quasi-regular codes [6],

$$\sum_{\mathbf{C}_l} P(\mathbf{c}_i) = \frac{1}{2^k} \tag{2.12}$$

Substitute (2.11) and (2.12) in (2.8)

$$P_e \leq \frac{1}{2}T(D) \tag{2.13}$$

The transfer function is a function of the variable D, which enumerates the distance of an error sequence from the correct one. Now, the path length enumerator L and input-bits enumerator I variables are added to the transfer function, and assuming quasi-regularity makes (2.11):

$$T(D, L, I) = \sum_{l=1}^{\infty} \sum_{\mathbf{E}_l \neq 0} L^l I^i \prod_{t \in \hat{\nu}} D \tag{2.14}$$

2.4.1 Modified Transfer Function

The transfer function in the form $T(D, L, I)$ does not show other characteristics such as the magnitude of protection on individual input bits (depending on their position), which is what this thesis is aiming for. To further study such characteristics, one must reside to a more descriptive representation. In this section, the transfer function $T(D, L, I)$ is going to be modified to reflect the weight of individual input bits. This will give us the ability to exactly measure the protection capabilities of ST codes on information bits depending on their position.

A convolutional code that takes more than one input bit offers natural *unequal error protection* to its input bits depending on their bit position [38]. Omura

and Simon [39] were the first to notice this property in a rate 2/3 convolutional code. Mills and Costello [38] modified the transfer function to calculate the error protection capabilities of convolutional codes. Here, a modified transfer function of (2.11) is presented to show the protection on individual input bits by replacing I^i with $I_1^{i_1} I_2^{i_2} \cdots I_k^{i_k}$, where $I_1, I_2, \ldots, I_k$ and $i_1, i_2, \ldots, i_k$ denote the individual input bits enumerators and the corresponding Hamming weight for a sequence of length l, respectively:

$$T(D, L, I_1, I_2, \ldots, I_k) = \sum_{l=1}^{\infty} \sum_{\mathbf{E}_l \neq 0} I_1^{i_1} I_2^{i_2} \cdots I_k^{i_k} L^l \prod_{t \in \hat{\nu}} D \tag{2.15}$$

This modified transfer function will be the main tool necessary to find codes that are strong in protecting one input bit without caring much about the other bit or even the overall performance of the code.

2.4.2 Bit Error Probability for Individual Input Bits

For a general trellis code, bit error probability is given by [6]:

$$P_b \leq \frac{\mathrm{C}(m, L)}{k} \cdot \frac{\partial T(D, I)}{\partial I}\bigg|_{I=1} \tag{2.16}$$

where $T(D, I)$ is the transfer function as a function of the distance D and input bits I. As mentioned earlier, the transfer function can be calculated from the distance spectrum. $\mathrm{C}(m, L)$ is a tightening constant derived by Zummo and Al-Semari and

is given by[25]:

$$\mathrm{C}(m,L) = \frac{1}{2^{2mL}} \sum_{j=1}^{mL} \binom{2mL-j-1}{mL-1} \left(\frac{2}{1+\sqrt{\phi_{\min}}} \right)^{j} \tag{2.17}$$

where L is the minimum time instances in which the codewords $\mathbf{c}_t = c_t^1 c_t^2 \ldots c_t^n$ are different from the all-zero codeword and

$$\phi_{\min} = \min \left\{ \frac{E_s \sum_{i=1}^{n} |c_t^i - \hat{c}_t^i|^2}{4N_0 + E_s \sum_{i=1}^{n} |c_t^i - \hat{c}_t^i|^2}, \qquad t \in \hat{\nu} \right\}$$

To find the BEP of individual input bits, consider the modified transfer function of Equation (2.15) in a manner similar to the work in [38]. The new upper-bound for individual input bits becomes:

$$P_b^{(i)} \leq \mathrm{C}(m,L) \cdot \frac{\partial T(D, L, I_1, I_2, \ldots, I_k)}{\partial I_i}\bigg|_{I_i=1} \tag{2.18}$$

where $P_b^{(i)}$ is the average BEP of the input bit i.

Example 2 *Consider the code of Figure 2.3, which was introduced in [1]. For the purpose of this example, let the code be quasi-regular (see Example 1 for proof). This code has two input bits to the encoder, I_1 and I_2. To demonstrate the unequal error protection properties of this code, the new upper-bound is calculated for each input bit. In addition, the same code is simulated over a rapid fading channel. It is clear from the plot in Figure 2.4 that I_1 is better error-protected than I_2.*

2.4.3 Distance Spectrum

From Equation (2.15), it can be seen that the transfer function $T(D, L, I)$ is a series that can be expanded for all values of the sequence-length l for the period $[0, \infty)$. Evaluating this series and finding the coefficients of each term is necessary for the calculation of an upper bound on bit error probability. The values of the coefficients, d, l and $i_1, i_2, \ldots, i_k$ can be found by expanding the trellis diagram of the code. In other words every possible path is enumerated and the all distances between all possible pairs of paths are calculated. This can be done by finding the *distance spectrum.*

Example 3 *For the same code of Example 2 (shown in Figure 2.3), the series of (2.15) is expanded to find the values of the coefficients, d, l, i_1 and i_2. Here, the all-zero codeword is assumed to be the correct transmitted codeword without loss of generality, since the code is quasi-regular. The distance spectrum of this code is shown in Table 2.2 and Figure 2.5. Its distance spectrum shows that for $l = 2$ and PD = 4, there is one path with Hamming weight of 1 for the first input bit I_1, while there are two paths with Hamming weight of 1 for the second input bit I_2. For $l = 2$ and PD = 16, I_1 has a Hamming weight of 1, while I_2 has a weight of 0. This indicates that I_1 is more error protected than I_2, which is consistent with the result from Example 2.*

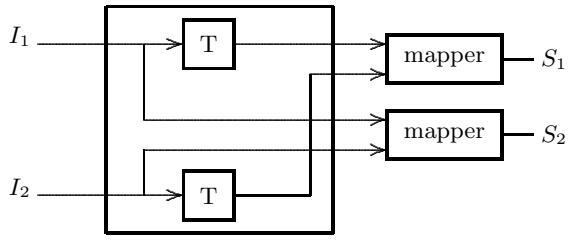

Figure 2.3: Encoder of the code in Example 2

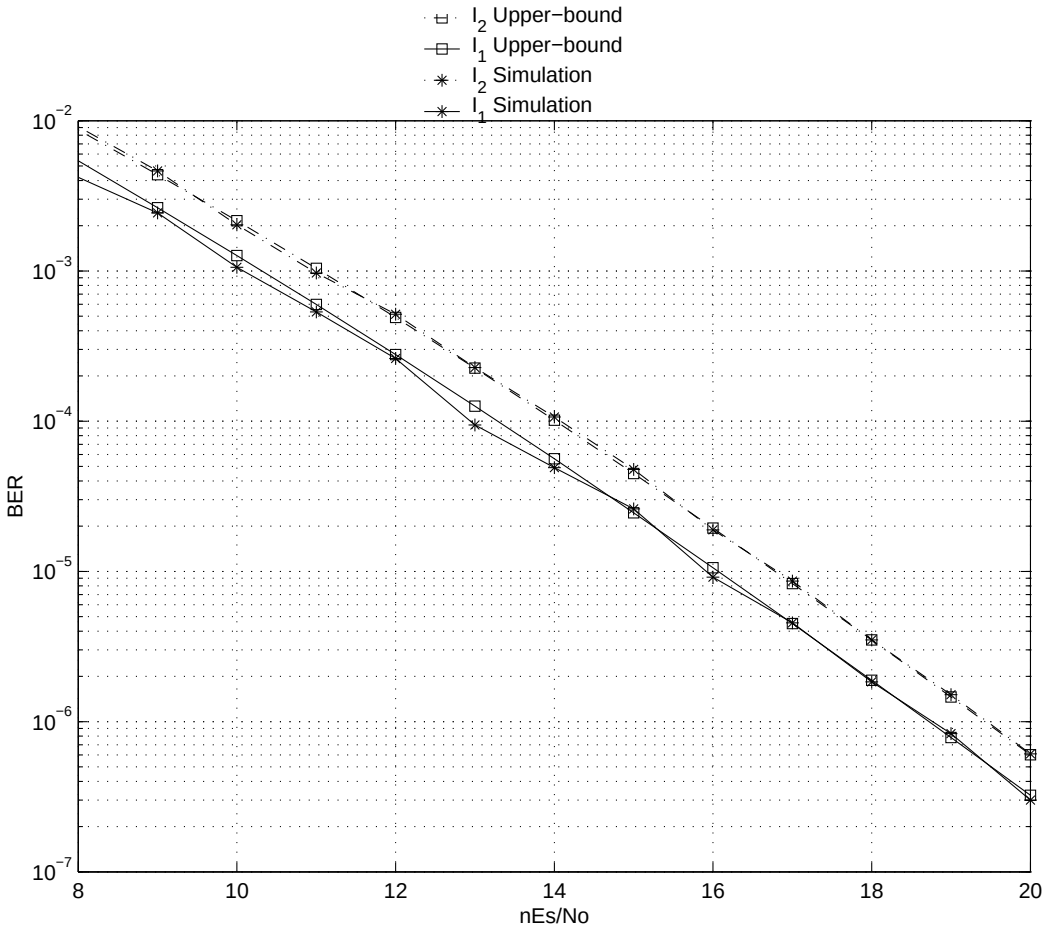

Figure 2.4: BEP upper-bound and simulation for I_1 and I_2 of the code in Example 2 ($m = 2$)

TABLE 2.2: DISTANCE SPECTRUM FOR THE CODE OF EXAMPLE 3

l	i_1	i_2	Product Distance
2	1	1	4
2	0	1	4
2	1	0	16
3	0	2	16
3	1	2	16
3	1	2	16
3	2	2	16
3	2	1	48
3	1	1	48
3	1	1	48
3	2	1	48
3	2	0	128
4	0	3	64
4	1	3	64
4	1	3	64
4	2	3	64
4	1	3	64
4	2	3	64
4	2	3	64
4	3	3	64
4	1	2	144
4	2	2	144
4	2	2	144
4	3	2	144
4	1	2	192
4	2	2	192
4	2	2	192
4	3	2	192
4	1	2	192
4	3	2	192
4	2	2	192
4	2	2	192
4	2	1	384
4	2	1	384
4	3	1	384
4	3	1	384
4	2	1	576
4	3	1	576
4	3	0	1024

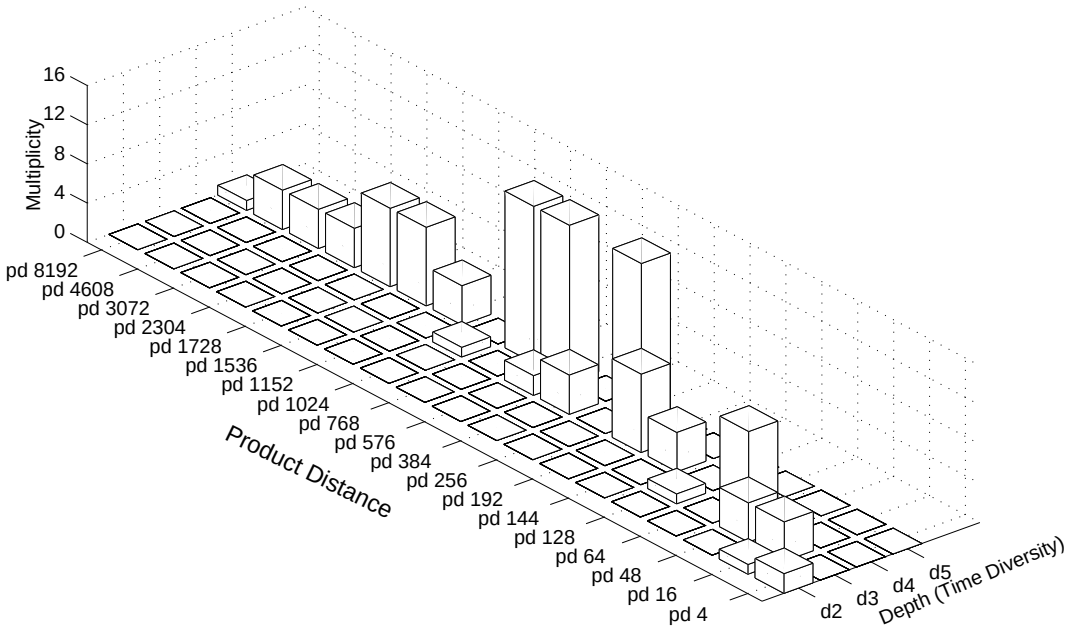

Figure 2.5: Distance Spectrum for Code of Example 3

2.5 QR AND NON-QR CODES PERFORMANCE EXAMPLES

The following two examples are of quasi-regular and non-quasi-regular ST trellis codes and their performance using both bounds presented previously (bound 1 from Equation (2.16) without the tightening constant and bound 2 with the tightening constant) and simulation over a rapid fading channel.

Example 4 *Consider the code in Figure 2.1. It was demonstrated in Example 1 that this code is quasi-regular. Therefore, bounds 1 & 2 can be applied assuming the all-zero codeword being transmitted without loss of generality. The transfer function* $\left.\frac{\partial T(D,I)}{\partial I}\right|_{I=1}$ *can be calculated from the expanded distance spectrum.*

The results are shown in Figure 2.6. It is clear from simulation results that the code is upper bounded by both bounds for the cases of one and two receive antennas.

Example 5 *Consider the code in Figure 2.7. Investigating the first condition of quasi-regularity shows that this code cannot be realized using a linear encoder, because it requires AND gates. Furthermore, this code does not abide with the second condition of quasi-regularity. For example* $P_{2,3,0100}$ *is defined for some but not all signals between the two states* σ_2 *and* σ_3*.*

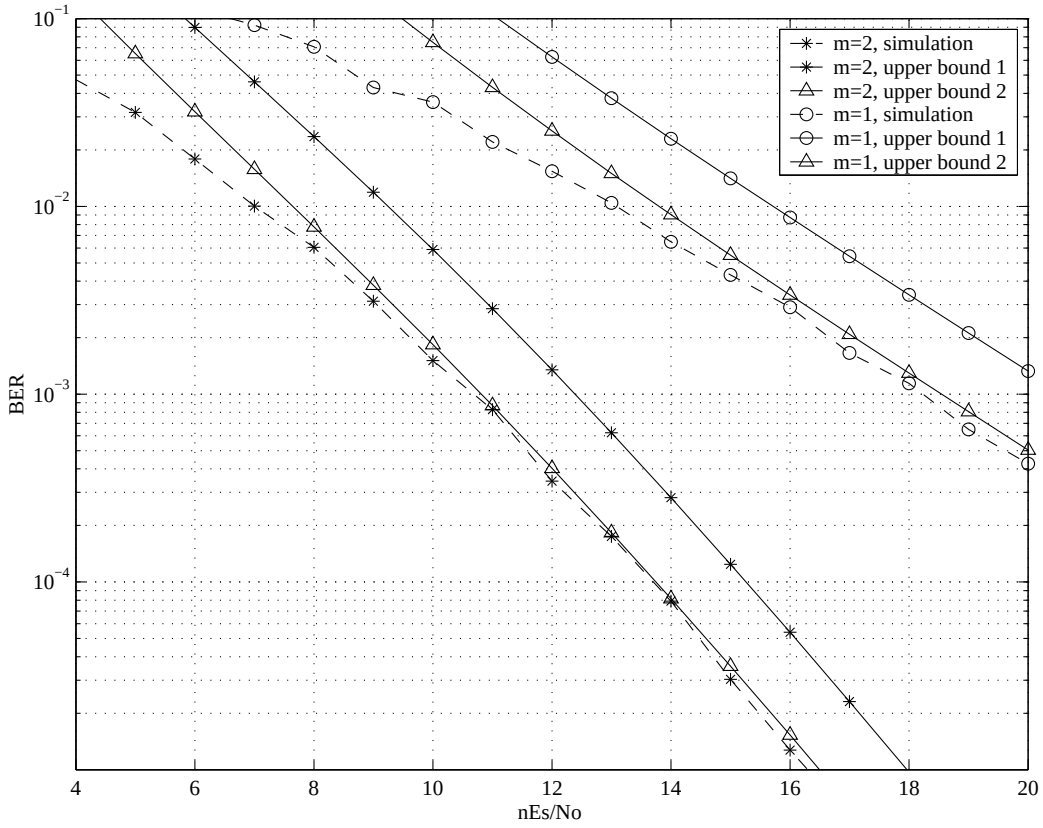

Figure 2.6: Code of Example 4 - simulation and upper bounds for m = 1 & 2

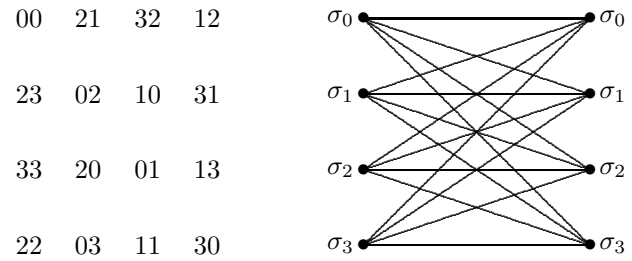

Figure 2.7: Non-quasi-regular code of Example 5

The simulation and upper bounds calculations are shown in Figure 2.8, which shows that this code is not upper bounded by the tighter bound of Equation (2.16) and hence showing its non-quasi-regularity.

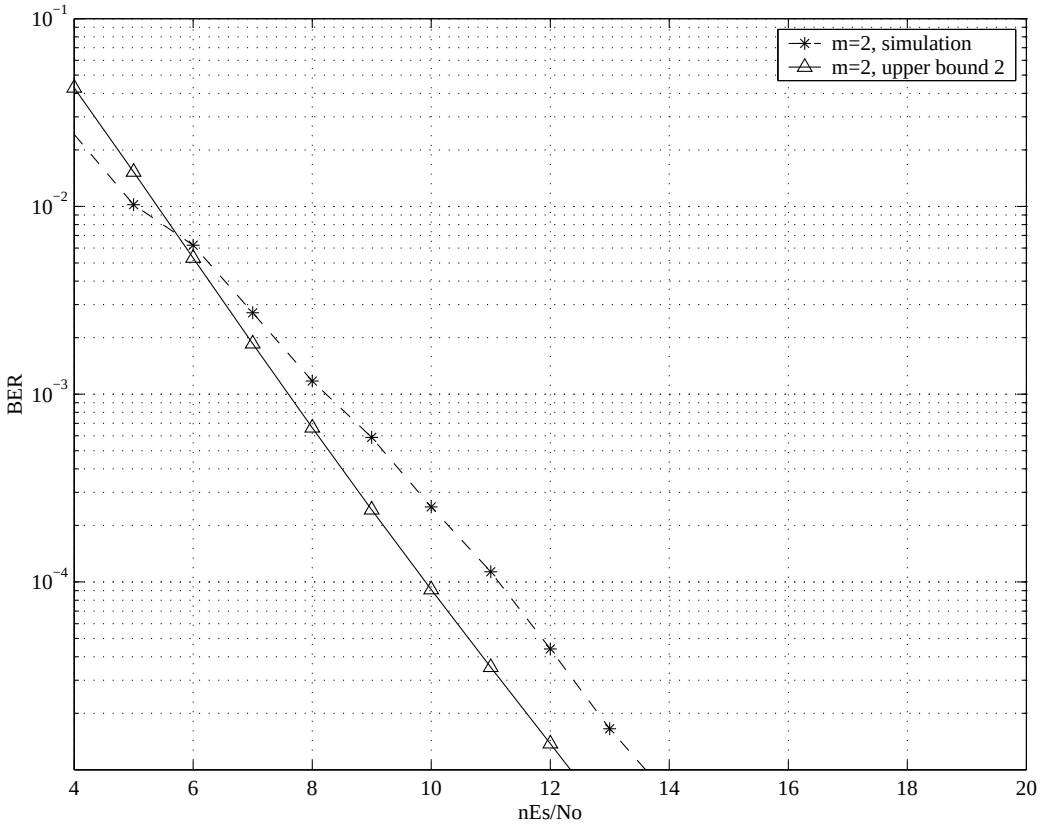

Figure 2.8: Code of Example 5 - simulation and upper bounds for m = 1

CHAPTER 3

DESIGN OF UEP ST TRELLIS CODES

3.1 INTRODUCTION

In Chapter 2 the tools necessary to find, design and evaluate ST trellis codes with unequal error protection were presented. In this chapter, those tools will be used to find and design codes that satisfy the goals of this thesis. As mentioned in Chapter 1, the image's bits can be divided into two categories (or more) according to importance. It is desirable that the more important part of the image has better error protection. Therefore, one can see that even a code of moderate overall error protection, but with strong error protection on one of its input bits can outperform a code of strong overall error protection, but with equal error protection on all of its input bits. In order to satisfy this goal, two approaches of code design and search are implemented. The first one is an *exhaustive search* of all possible codes

with N states and a certain modulation scheme. The search criteria is built on the modified performance evaluation tools presented previously that show the weight of different input bits. The second approach is *code design* using a new design approach that ensures that the code gives more protection to the most significant bit (MSB). All codes designed through these two approaches are simulated and compared to codes from the literature to evaluate their performance.

3.2 Exhaustive Search Approach

The first step in the exhaustive search approach is code generation. After generating all possible codes, the codes are searched to find the best ones satisfying the proposed search criteria. Finally, the chosen codes are simulated to check their performance and see if they satisfy the expectations.

3.2.1 Code Generation

In order to generate all possible ST trellis codes of a certain number of states and modulation scheme, one must reside to a representation other than the trellis representation. The reason is that the trellis representation is very general. For example, it includes non-linear codes which are beyond the scope of this thesis. One possible alternative representation is described in the following.

Let $\mathbf{I}$ be a binary vector of input bits defined as

$$\mathbf{I} = \mathbf{i}_0 \mathbf{i}_1 \cdots \mathbf{i}_t$$

where

$$\mathbf{i}_t = i_t^{k+j}\ i_t^{k+j-1} \cdots i_t^0$$

where k is the number of input bits to the encoder in parallel and j is the number of memory elements. Let $\mathbf{G}$ be a generator matrix of size $(k+j) \times (n\tilde{n})$ where $n\tilde{n}$ is the number of encoded bits. Each entry in $\mathbf{G}$ is either 0 or 1 depending on the presence or absence of a connection between the output bits and the input bits. If a column has more than one entry of 1, it the connections are combined using modulo-2 addition. The reason of using a modulo-2 adder is to ensure the linearity of the encoder which is a quasi-regularity requirement. The corresponding binary encoded-bits vector at time t $\mathbf{a}_t = a^{n\tilde{n}}\ a_t^{n\tilde{n}-1} \cdots a_t^0$ is given by:

$$\mathbf{a}_t = \mathbf{i}_t \cdot \mathbf{G} \tag{3.1}$$

To demonstrate this, consider the code of Figure 2.1. This code has 2 memory elements ($j = 2$), 2 input bits ($k = 2$) and 4 output bits ($n\tilde{n} = 4$). For this code, the generator matrix $\mathbf{G}$ is given by:

$$\mathbf{G} = \begin{pmatrix} 0 & 0 & 1 & 0 \\ 0 & 0 & 0 & 1 \\ 1 & 0 & 0 & 0 \\ 0 & 1 & 0 & 0 \end{pmatrix}$$

The generator matrix representation is a direct mapping from the circuit representation. This can be seen by comparing the previous example of $\mathbf{G}$ and the circuit representation of the code shown in Figure 2.3.

Using this representation, all possible *linear* codes (for a given $n\tilde{n}$, k and j) can be generated by having all possible combinations of $\mathbf{G}$. The trellis representation of a certain code can be produced by mapping the output binary codewords $\mathbf{a}$ of all possible different input sequences using a one-to-one mapping function μ.

3.2.2 Code Search Criteria

After generating all possible codes with certain $n\tilde{n}$, k and j, it is necessary to define the criteria for choosing the best codes. As pointed out earlier in this chapter, the goal of this thesis is to find codes that provide strong error protection to the MSB. To accomplish this task for quasi-regular codes, it is possible to depend on the modified distance spectrum described in Chapter 2. The reason why the conventional distance and product criteria are not used in their original form is that they do not reflect the weight of protection on different input bits. Furthermore, for codes with equal minimum symbol-differences and minimum product distance properties, it is necessary to go to higher product distances. The modified distance

spectrum shows the symbol differences, product distance and the Hamming weight of every input bit individually.

In order to find codes of strong error protection on one input bit, it is necessary to apply the following rules in the search:

1. The minimum symbol-differences are maximized with respect to the MSB.
2. The minimum product distance is maximized with respect to the MSB.
3. Higher product distances are maximized with respect to the MSB.
4. Inter-codeword squared Euclidean distances (SED) in each state are maximized.
5. Codes that do not span the whole codewords spectrum are not considered.

It is necessary to follow the above rules in the same order. Items 1 and 2 are modified distance and product criteria to reflect unequal error protection on different input bits. Items 3 and 4 come second in importance in the search criteria. Item 5 is a condition to reject codes that do not span the whole codeword spectrum (16 and 64 codewords for QPSK and 8PSK, respectively). Such codes are obviously weak in performance.

3.3 Design Approach

In order to handcraft a code, the design criteria should be laid out first before describing the design steps. The design requirements are very similar to the ones described earlier in the search criteria.

One of the effective design approaches of space-time trellis codes over rapid fading channels described in the literature is the one devised by Zummo and Al-Semari [10] and [40]. Their method is built on the multidimensional M-PSK set partitioning of trellis codes over fading channels described in [41]. The basic idea is to partition all possible signal combinations in a step by step manner. In each partitioning instance, certain properties (such as the symbol-wise Hamming distance and the inter-signal SED) are maximized. The partitioning is repeated until those properties can no longer be maximized. The results are good performing codes over rapid fading channels for both trellis codes and ST trellis codes (see [10], [40] and [41]).

Although the set partitioning method is appealing, it is not suitable for the purpose of this work because it does not take the weight of input bits into account. Therefore, a new design method is proposed in the following that solves this problem and takes the weight of error protection on each input bit into consideration.

Before going into the design steps of the new method, general observations should be considered first:

- All designed codes should be quasi-regular.

- Not all codewords are the same in terms of importance, because their SED's from the all-zero codeword are different.
- The position of the codeword in the trellis diagram is connected to the position of the input bit.
- The key to increase the product criterion for a certain input bit is by assigning codewords with the highest Euclidean distances to positions related to that input bit.
- State σ_0 is considered the most important state, because it is the initial state of the encoder.

The proposed new design steps, based on the previous observations and guidelines, are:

1. Distances properties of input bits should be examined first to check their minimum time diversity property. If one has better diversity properties, it should be chosen as the MSB. Otherwise, any input bit would be a fair choice.
2. Codewords with the best distance properties should be identified.
3. The connection between the position of the input bits and the position of the codewords in the trellis diagram should be identified.
4. To determine which positions of codewords are more important for the minimum product distance, the trellis diagram should be expanded for the few

minimum possible transmitted sequences.

5. The best codewords are assigned to the important positions connected to the MSB which were determined in Steps (2)-(4) such that:

   (a) State σ_0's important positions are chosen from the best codewords.

   (b) The minimum inter-codeword SED of state σ_0 should be maximized.

   (c) The important codeword positions in the remaining states are chosen from the best codewords.

   (d) Symmetry is maintained in the trellis diagram.

6. Modulo-2 addition of the codewords' binary labels is used to derive the remaining codewords in the following manner while maintaining symmetry:

   (a) The remaining codewords in state σ_0 are derived from the chosen ones.

   (b) The remaining states' codewords are derived from state σ_0.

7. Ensuring quasi-regularity of the designed code is a priority over the choice of good codewords' positions in the trellis diagram. Therefore, if the best choice of codewords' positions produces a non-quasi-regular code, the codewords should be re-arranged such that the code is quasi-regular.

Condition (1) is the modified version of the distance criterion. Conditions (5a) and (5c) are to maximize the minimum product distance of the MSB, which is the modified version of the product criterion. Conditions (5d) and (6) are to satisfy

the two conditions of quasi-regularity. Finally, condition (5b) is to enhance the performance of the code in general in a manner similar to the set partitioning procedure. As will be shown in the following section, the above rules are applied to handcraft QPSK codes that perform well for the MSB.

3.4 Search and Design-Based Codes

In this section, the proposed 7-step design method and the search criteria are applied to 4, 8 and 16-state QPSK and 8-state 8PSK.

Before going into the resulting codes, a few notes are necessary to clear the search and design results:

- Code search and design results are not unique. There are many variations for the chosen codes that give identical results. The reason is that they have identical properties, and any possible further distinguishing factor is done through simulation.

- The QPSK codes' rate is 2 b/s/Hz while the 8PSK's rate is 3 b/s/Hz. This rate difference should be considered when code performance comparisons between QPSK and 8PSK codes are made.

- Having more constellation points in th 8PSK codes reduces the SED's between codewords, which in turn reduces the general performance of them.

- Increasing the number of memory elements and hence the number of states enhances the protection of the MSB and the overall performance of the code.
- The two approaches aim to give maximum error protection to the MSB only and ignore the least significant bits (LSB). This makes the overall performance of the new codes inferior to the best codes in the literature.
- Unlike the set partitioning method, the proposed design method does not make the state minimum inter-codeword SED a priority. Therefore, in general, it is smaller in the new codes than the best ones in literature, which decreases the overall performance.
- Exhaustive search scope is 16^4 for 4-state QPSK, 32^4 for 8-state QPSK, 64^4 for 16-state QPSK and 64^6 for 8-state 8PSK codes.
- From looking at fully connected codes (e.g. 4-state QPSK and 8-state 8PSK), one can notice that the distance criterion cannot be increased, even for a single input bit. In certain cases of not-fully connected codes however, certain input bits may have better distance properties than others (see the case of 8-state QPSK later in the this section).

3.4.1 Search-Based Codes

The first approach to find codes that meet the goal of UEP is the comprehensive code search approach. In order to apply the search criteria described in section

3.2, a C language program has been designed to generate and search all possible 4, 8 and 16-state QPSK codes with a linear encoder and find the best ones that meet the criteria. The search results for 4, 8 and 16-state QPSK codes are shown in Figure 3.1. The search result for 8-state 8PSK codes is shown in Figure 3.2. The generator matrices of the search based codes are shown in Figure 3.3

3.4.2 Design of 4-State QPSK Codes

The 4-state code is fully connected. Therefore the minimum time diversity for both bits is 2 in all possible codes. The next distinguishing factor is the product distance.

The first step in the design is picking which input bit to have better error protection. Since the two input bits I_0 and I_1 have the same minimum time diversity properties, either one can be chosen. The second step is to identify codewords with the highest SED's from the all-zero codeword. Table 3.1 shows the QPSK constellation points and the SED's of all possible codewords (denoted by CW) from the all-zero codeword. From the table, the codewords with the highest SED's from the all zero codeword are 22, 12, 21, 23 and 32. As per the third step, Figure 3.5 identifies the association of the codewords in the trellis diagram with the input bits for 4-state QPSK. For Step 4, Figure 3.6 identifies all possible paths of depth 2, their product distances and their input bits association.

Let I_0 be the MSB choice here, it can be seen from Figure 3.6 that 1^{st} and 3^{rd}

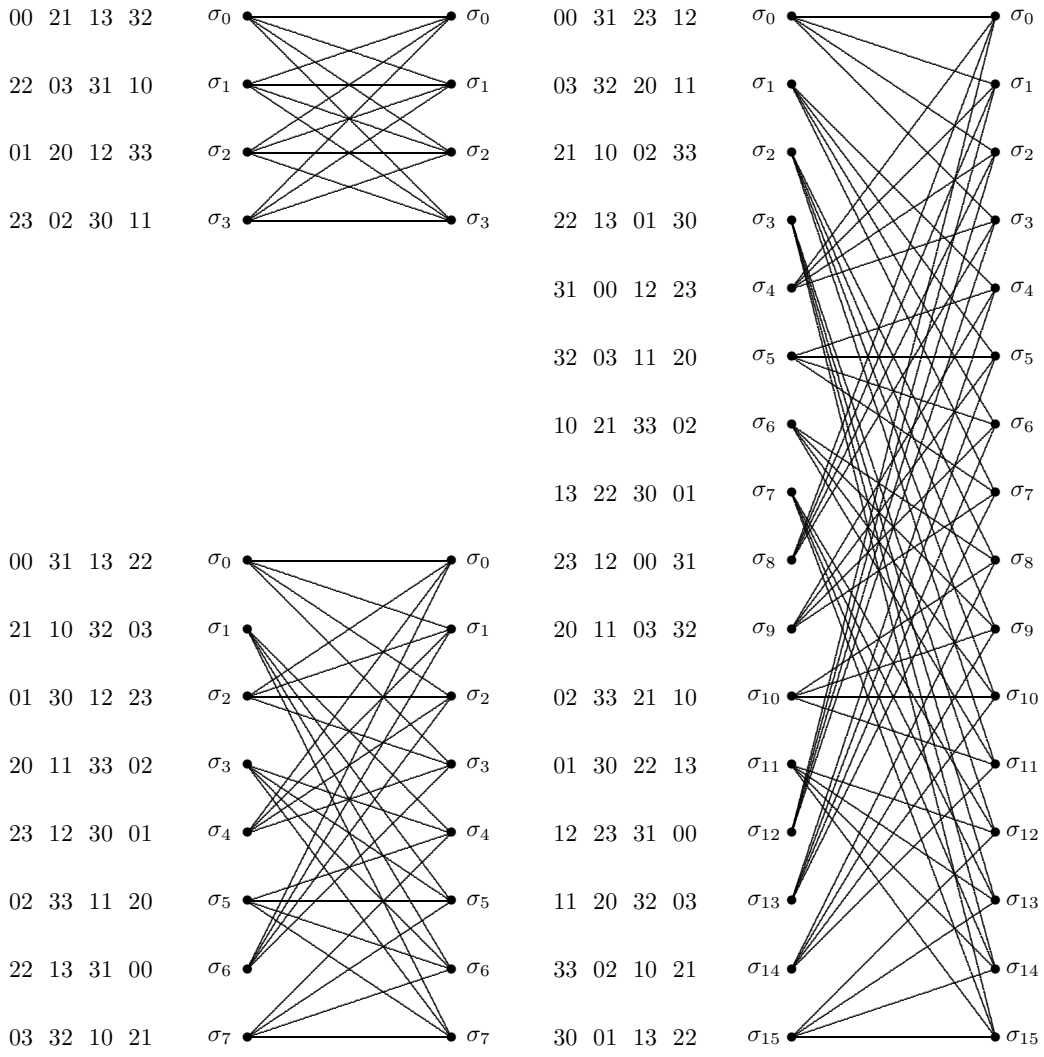

Figure 3.1: QPSK search based codes

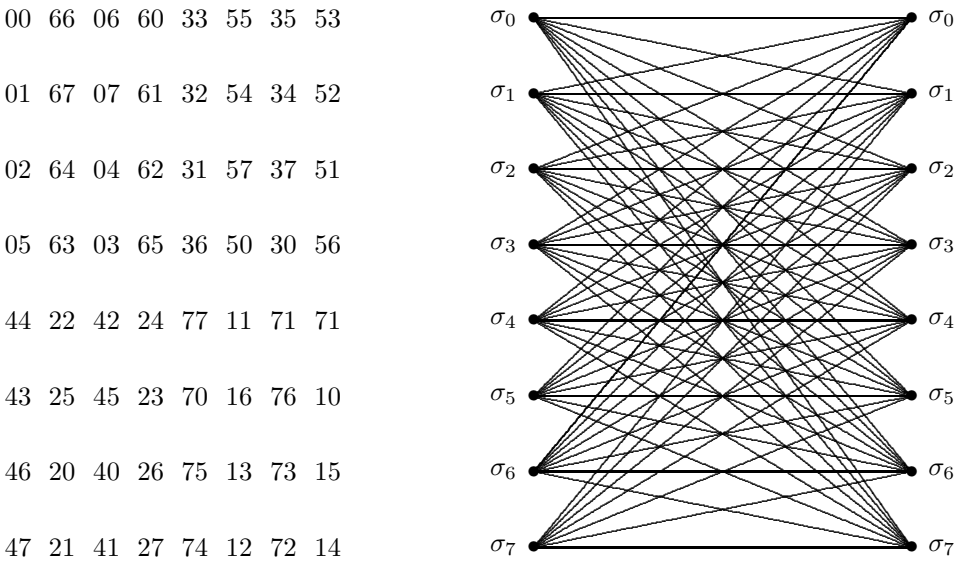

Figure 3.2: 8PSK search based code

$$\begin{pmatrix} 0 & 1 & 1 & 1 \\ 1 & 0 & 0 & 1 \\ 0 & 0 & 0 & 1 \\ 1 & 0 & 1 & 0 \end{pmatrix}$$

(a) 4-state QPSK

$$\begin{pmatrix} 0 & 1 & 1 & 1 \\ 1 & 1 & 0 & 1 \\ 1 & 0 & 1 & 1 \\ 0 & 0 & 0 & 1 \\ 1 & 0 & 0 & 1 \end{pmatrix}$$

(b) 8-state QPSK

$$\begin{pmatrix} 1 & 0 & 1 & 1 \\ 1 & 1 & 0 & 1 \\ 1 & 0 & 1 & 1 \\ 1 & 1 & 0 & 1 \\ 1 & 0 & 0 & 1 \\ 0 & 0 & 1 & 1 \end{pmatrix}$$

(c) 16-state QPSK

$$\begin{pmatrix} 0 & 1 & 1 & 0 & 1 & 1 \\ 0 & 0 & 0 & 1 & 1 & 0 \\ 1 & 1 & 0 & 1 & 1 & 0 \\ 1 & 0 & 0 & 1 & 0 & 0 \\ 0 & 0 & 0 & 0 & 1 & 0 \\ 0 & 0 & 0 & 0 & 0 & 1 \end{pmatrix}$$

(d) 8-state 8PSK

Figure 3.3: Generator matrices $\mathbf{G}$ of the search-based codes

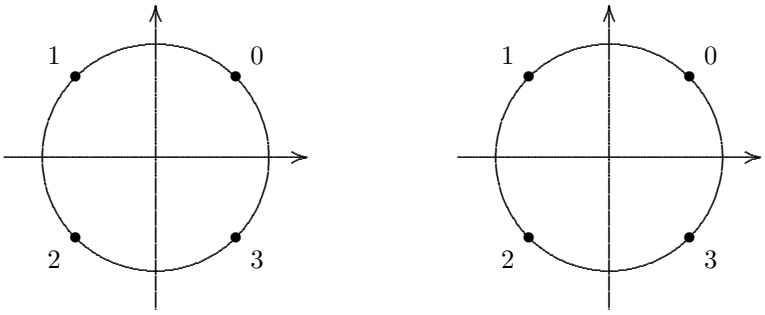

Figure 3.4: QPSK signal constellation

TABLE 3.1: CODEWORDS' SED'S FROM THE ALL-ZERO CODEWORD FOR QPSK CODES

CW	SED	CW	SED	CW	SED	CW	SED
00	0.0	10	2.0	20	4.0	30	2.0
01	2.0	11	4.0	21	6.0	31	4.0
02	4.0	12	6.0	22	8.0	32	6.0
03	2.0	13	4.0	23	6.0	33	4.0

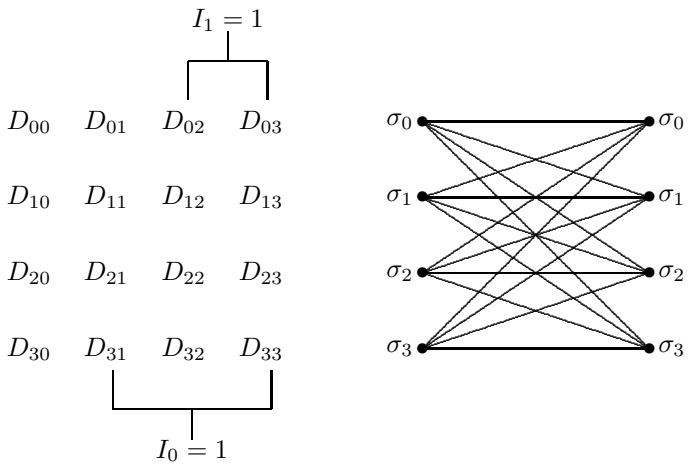

Figure 3.5: QPSK 4-state input-bits association

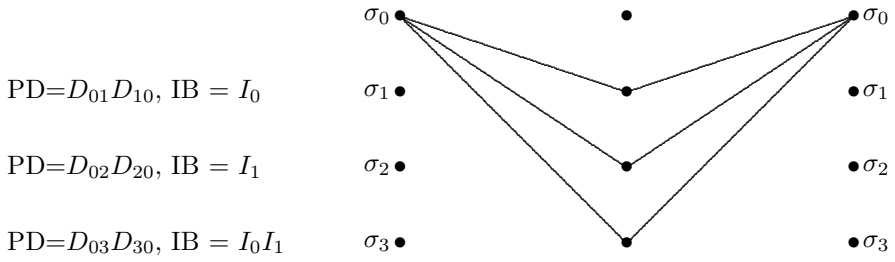

Figure 3.6: Depth 2 possible path combinations with product distances and input bits assignment for 4-state QPSK codes

paths are the ones to be improved in terms of minimum product distance. The SED pointers associated with these two paths are D_{01}, D_{10}, D_{03} and D_{30}. These pointers should be assigned codewords that have higher SED values, which were determined earlier in the second step. In Step 5, the initial codeword assignment, the important pointers D_{01} and D_{03} in state σ_0 are chosen from the best codewords such that the state minimum inter-codeword SED is maximized. Also, the remaining important pointers D_{10} and D_{30} are chosen from the best codewords. This choice, shown in Figure 3.7, insures that the minimum product distance of I_0 is maximized. It must be stressed at this point that these are initial positions and are subject to change at any point depending on the outcome of the design. Furthermore, different designs producing different codes are possible depending on the designer's initial choice of the codewords' positions. Nevertheless, if all design criteria are satisfied, different codes will have identical performance.

As per Step 6, the rest of the codewords in state σ_0 are generated. As mentioned earlier in this chapter, half the codewords in state σ_0 are sufficient to produce the rest. Since the chosen ones are 21 and 23, they produce 02, which is the modulo-2 addition of their binary labels. According to this initial codeword position choice, the minimum product distance of I_0 is 36 and the minimum inter-codeword SED is 4. The remaining states' codewords are generated while keeping the condition of maintaining symmetry. Modulo-2 addition of the binary labels is used to produce the codewords of the remaining states such that Codewords 32, 10 and 22 are at

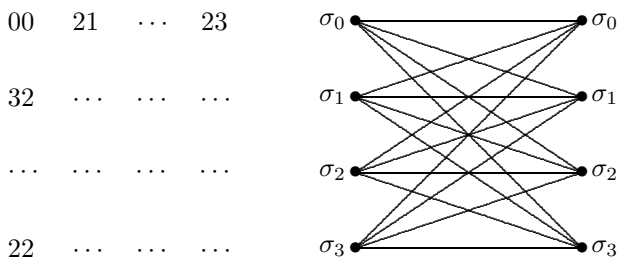

Figure 3.7: Initial Design Assignment

the first codeword position at states σ_1, σ_2 and σ_3, respectively. The resulting code is shown in Figure 3.8 for the trellis representation and in Figure 3.9 for the generator matrix representation. This choice of codewords ensures maximizing the minimum product distance for I_0 and ensures linearity of the encoder.

3.4.3 Design of 8 and 16-State QPSK Codes

Unlike the 4-state codes, the 8 and 16-state codes are not fully connected. This makes it possible to have minimum time diversity greater than 2 for the MSB. In the case of 8-state codes, the first input bit has a minimum time diversity of 3, while the second input bit has minimum time diversity being 2, as shown in Figure 3.10. This makes I_0 have better error protection than I_1 in all possible codes and should be the MSB choice. However, in the case of 16-state codes, both input bits have minimum time diversity of 3 (see Figure 3.11).

The same 7-step procedure used before for 4-state QPSK is repeated to produce the 8 and 16-state QPSK codes shown in Figures 3.8 and 3.9.

3.4.4 Design of 8-State 8PSK Codes

Like 4-state QPSK, 8-state 8PSK is fully connected. This makes the minimum time diversity be 2 for all possible codes and all possible input bits.

The same steps used before to design QPSK codes are applied here again to design 8-state 8PSK codes. Since all three input I_0, I_1 and I_2 bits have the same

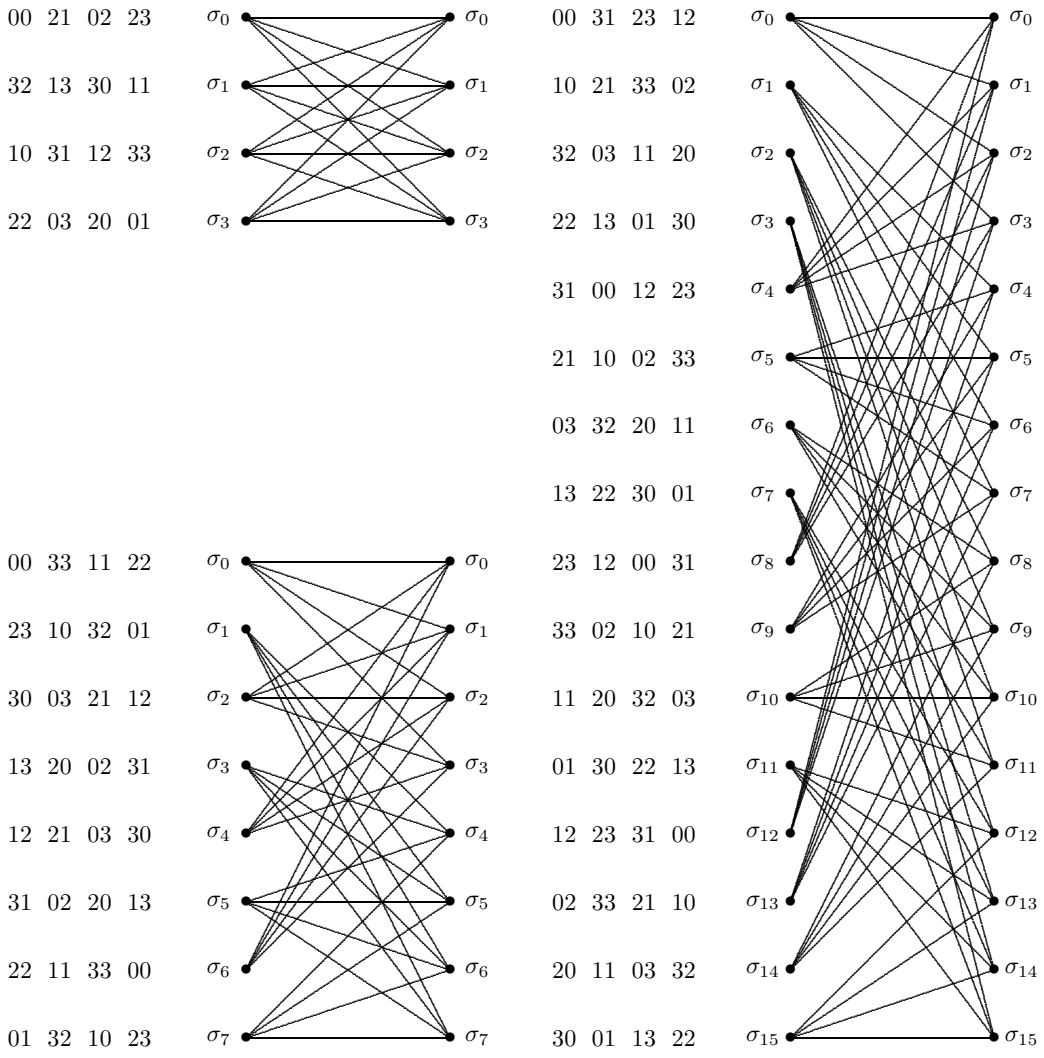

Figure 3.8: Design-based codes: QPSK 4, 8 and 16-state

$$\begin{pmatrix} 0 & 0 & 1 & 0 \\ 1 & 0 & 0 & 1 \\ 0 & 1 & 0 & 0 \\ 1 & 1 & 1 & 0 \end{pmatrix}$$

(a) 4-state QPSK

$$\begin{pmatrix} 0 & 1 & 0 & 1 \\ 1 & 1 & 1 & 1 \\ 0 & 1 & 1 & 0 \\ 1 & 1 & 0 & 0 \\ 1 & 0 & 1 & 1 \end{pmatrix}$$

(b) 8-state QPSK

$$\begin{pmatrix} 1 & 0 & 1 & 1 \\ 1 & 1 & 0 & 1 \\ 1 & 0 & 1 & 1 \\ 1 & 1 & 0 & 1 \\ 1 & 1 & 1 & 0 \\ 0 & 1 & 0 & 0 \end{pmatrix}$$

(c) 16-state QPSK

Figure 3.9: Generator matrices $\mathbf{G}$ of the design-based codes

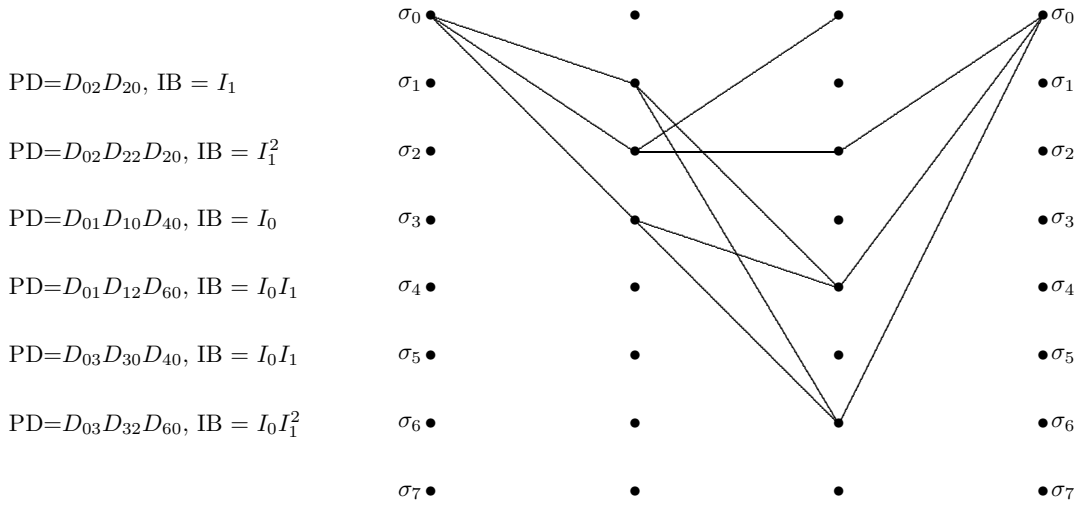

Figure 3.10: Depth 2 and 3 possible path combinations with product distances and input bits assignment for 8-state QPSK codes

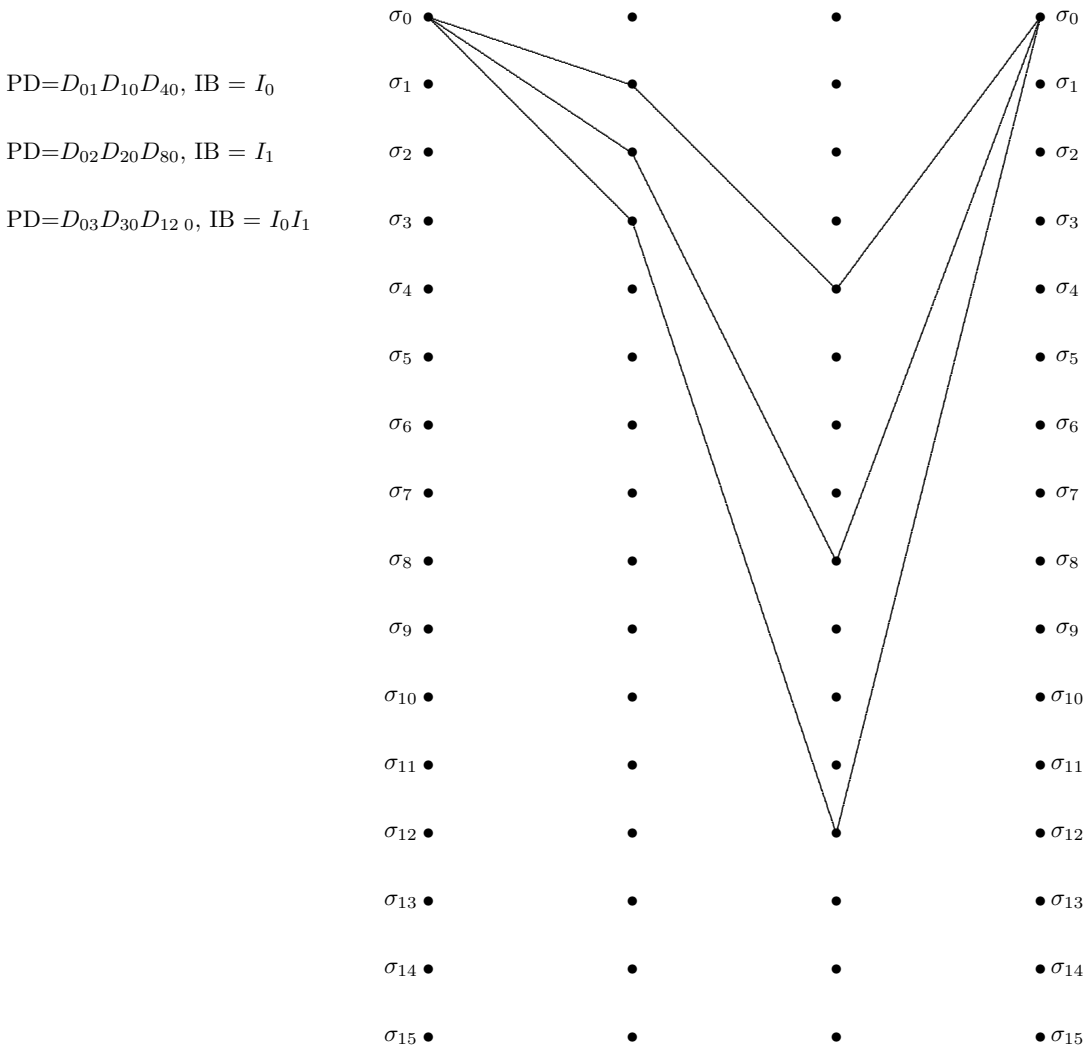

Figure 3.11: Depth 3 possible path combinations with product distances and input bits assignment for 16-state QPSK codes

minimum time diversity properties, any of them can be chosen to be the MSB. In the following work the choice is I_2. The 8PSK signal constellation points and the SED from the all-zero Codeword are shown in Figure 3.12 and Table 3.2. Figure 3.13 identifies the association of trellis diagram codewords with input bits for 8-state 8PSK. Furthermore, Figure 3.14 identifies all paths of depth 2, their product distances and their input bits association.

It can be seen from Figure 3.14 that the fourth to the eighth paths are the ones to be improved in terms of maximizing the minimum product distance. The Euclidean distance pointers associated with these four paths are D_{04}, D_{40}, D_{05}, D_{50}, D_{06}, D_{60}, D_{07} and D_{70}. The places of these pointers in the trellis diagram should be assigned codewords that have higher SED values. From Table 3.2, the codewords with the highest SED's from the all-zero Codeword are 44, 43, 34, 54, 45, 33, 55, 35 and 53. The next step is chose their initial positions in the trellis diagram so that the minimum product distance of I_2 and the state inter-codeword minimum SED are maximized, as shown in Figure 3.15. Again, this choice is not final, it might end up being a good choice, or it might need to be changed.

The next step is to generate the rest of the codewords in state σ_0. As mentioned earlier in this chapter, half the codewords in state σ_0 are sufficient to produce the rest. Since the chosen ones are 33, 55, 35 and 53, they produce 66, 06 and 60, which are the modulo-2 addition of the chosen codewords' binary labels. According to this initial codeword position choice, the minimum product distance of I_2 is 50.3 and

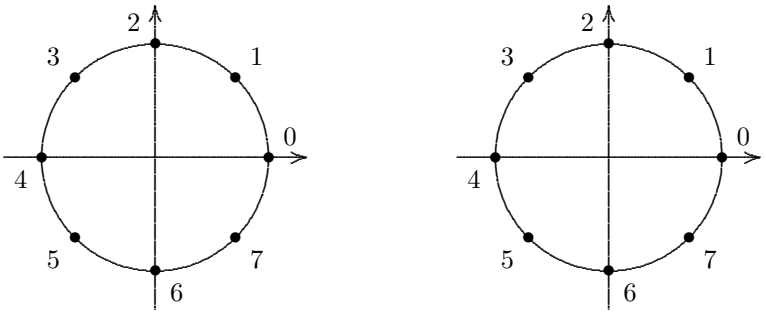

Figure 3.12: 8PSK signal constellation

TABLE 3.2: CODEWORDS' SED'S FROM THE ALL-ZERO CODEWORD FOR 8PSK CODES

CW	SED	CW	SED	CW	SED	CW	SED
00	0.0	20	2.0	40	4.0	60	2.0
01	0.6	21	2.6	41	4.6	61	2.6
02	2.0	22	4.0	42	6.0	62	4.0
03	3.4	23	5.4	43	7.4	63	5.4
04	4.0	24	6.0	44	8.0	64	6.0
05	3.4	25	5.4	45	7.4	65	5.4
06	2.0	26	4.0	46	6.0	66	4.0
07	0.6	27	2.6	47	4.6	67	2.6
10	0.6	30	3.4	50	3.4	70	0.6
11	1.2	31	4.0	51	4.0	71	1.2
12	2.6	32	5.4	52	5.4	72	2.6
13	4.0	33	6.8	53	6.8	73	4.0
14	4.6	34	7.4	54	7.4	74	4.6
15	4.0	35	6.8	55	6.8	75	4.0
16	2.6	36	5.4	56	5.4	76	2.6
17	1.2	37	4.0	57	4.0	77	1.2

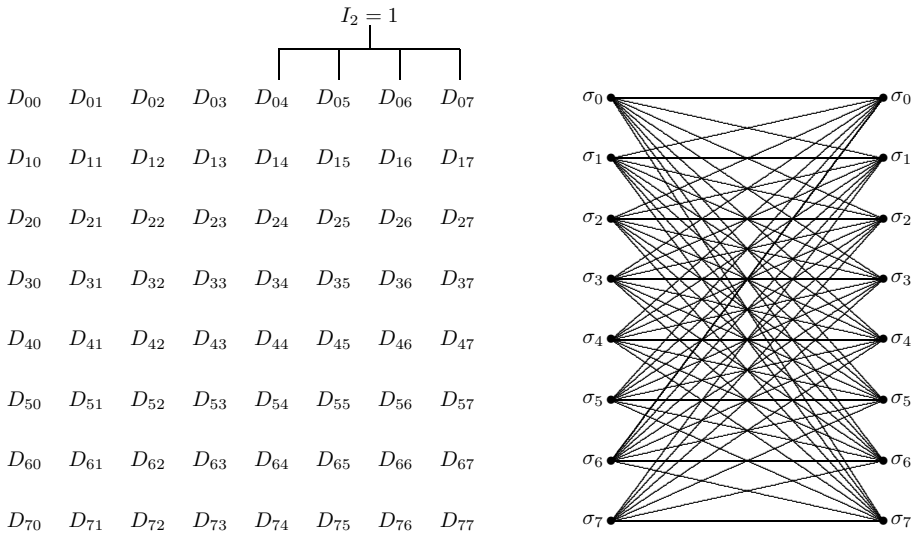

Figure 3.13: 8PSK 8-state input-bit I_2 association

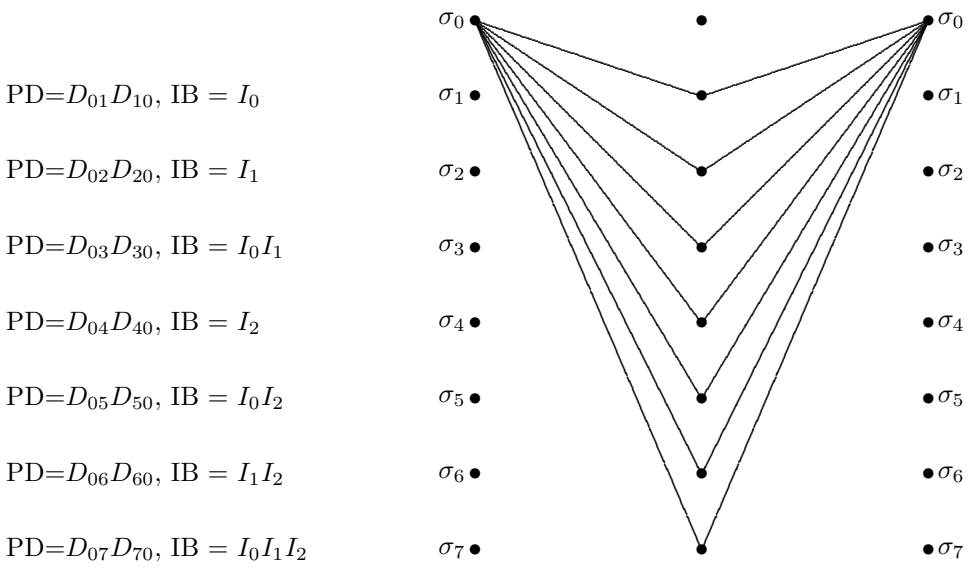

Figure 3.14: Depth 2 possible path combinations with product distances and input bits assignment for 8-state 8PSK codes

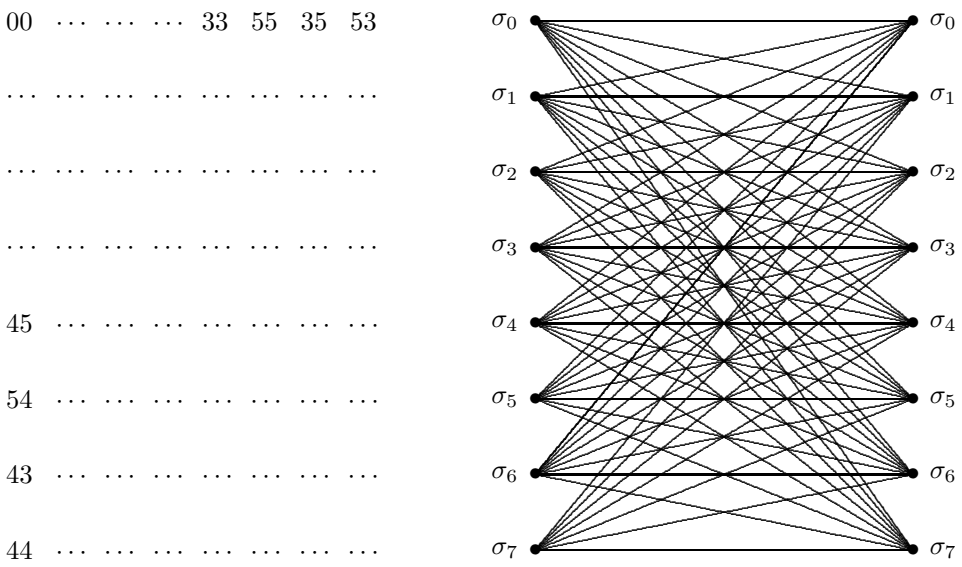

Figure 3.15: 8PSK initial design assignment

the minimum inter-codeword SED is 1.2. Modulo-2 addition of the binary labels is used to produce the codewords of the remaining states such that Codewords 46, 54, 43 and 44 are at the first codeword position at States 4 through 7, respectively. The result is shown in Figure 3.16.

Finally, the code must be checked for quasi-regularity. It can be seen from first transmit antenna's output in all 8-state that there are four 4's but only three 0's and one 5, which indicates asymmetry. This code requires a non-linear convolutional encoder, which makes it a non-quasi-regular code. Furthermore, it can be proven through simulation that this code does not perform to its expectations. Rearranging the codewords, to force the encoder's linearity gives the code shown in Figure 3.17 (Figure 3.18 for generator matrix representation). Although according to the distance spectrum of this code, it performs worse than the one in Figure 3.16 (minimum product distance for I_2 is 31.3 compared to 50.3), its simulation is much better.

3.5 New Codes Performance

Table 3.3 shows minimum product distance comparison of the MSB and LSB for the new codes and various codes from the literature. It is clear that there is a significant increase in the minimum product distance for the MSB In the new codes (design and search-based) compared to the ones in the literature. This is proven in the simulation plots shown in Figures 3.19, 3.20, 3.21 and 3.22 which

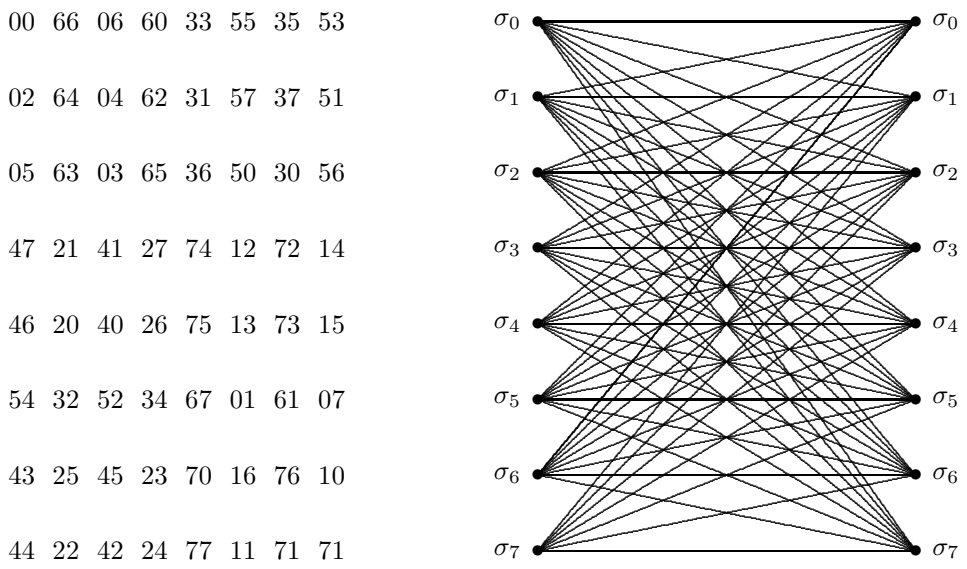

Figure 3.16: 8PSK second design assignment

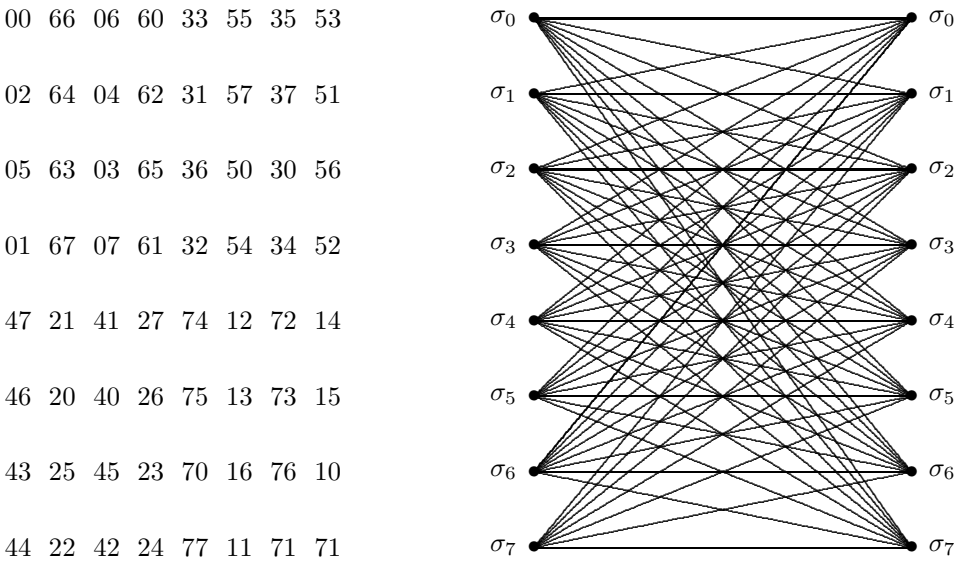

Figure 3.17: 8-state 8PSK design-based code

$$\begin{pmatrix} 0 & 1 & 1 & 0 & 1 & 1 \\ 0 & 0 & 0 & 1 & 1 & 0 \\ 1 & 1 & 0 & 1 & 1 & 0 \\ 1 & 0 & 0 & 1 & 1 & 1 \\ 0 & 0 & 0 & 1 & 0 & 1 \\ 0 & 0 & 0 & 0 & 1 & 0 \end{pmatrix}$$

Figure 3.18: Generator matrices $\mathbf{G}$ of the 8-state 8PSK design-based codes

show an improvement for the MSB in the new codes compared to other codes in the literature. As for the LSB, there is a decline in the minimum product distance properties, which shows in the simulation plots. This is expected since, as was mentioned earlier, the MSB was the center of focus, while the LSB was ignored totally in the two approaches. The plots show simulation for the designed codes only, because results are identical for both design and search-based codes. The improvement is relatively low at low SNR values, but the gain increases at high SNR. The largest gain is for the QPSK 8-state code, which gives a gain of more than 1.5 dB over the nearest code at a bit error rate BER = 10^{-5}. On the other hand, the smallest gain is for the 8-state 8PSK code, which is around 0.5 dB at BER = 10^{-5}. In the cases of 4 and 16-state QPSK, the gain is around 1.0 and 0.75 dB at BER = 10^{-5}, respectively.

TABLE 3.3: MINIMUM PRODUCT DISTANCE OF THE MSB AND LSB FOR VARIOUS CODES

		F-V-Y	Z-S	New (design)	New (search)
	4s QPSK	32.0	32.0	36.0	36.0
M	8s QPSK	32.0	96.0	144.0	144.0
S	16s QPSK	96.0	N/A	216.0	216.0
B	8s 8PSK	N/A	10.4	31.3	31.3
	4s QPSK	24.0	24.0	8.0	8.0
L	8s QPSK	48.0	24.0	8.0	8.0
S	16s QPSK	64.0	N/A	32.0	32.0
B	8s 8PSK	15.5	10.4	6.8	6.8

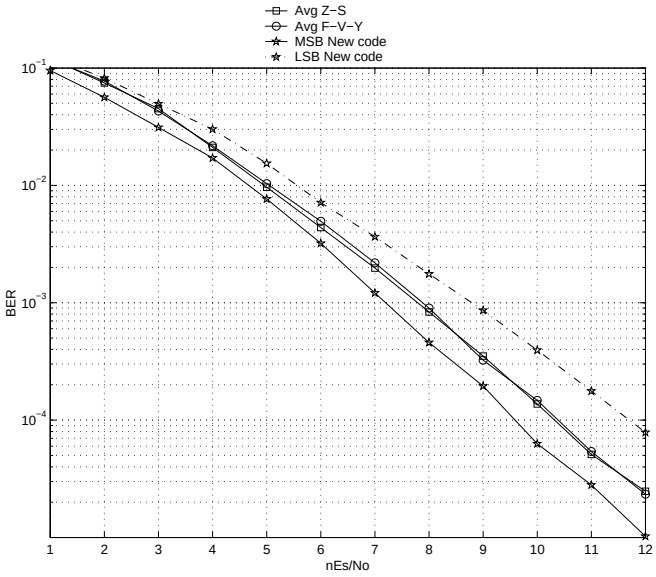

Figure 3.19: Simulation results for the new codes and codes from the literature (QPSK 4-state, 2 receive antennas)

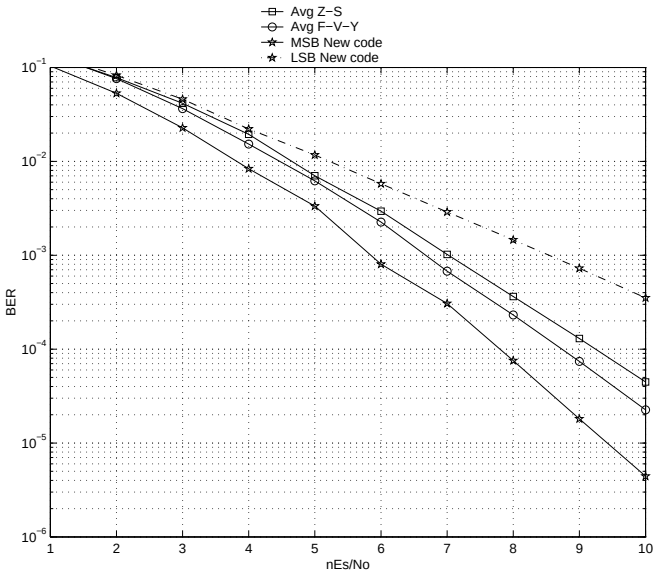

Figure 3.20: Simulation results for the new codes and codes from the literature (QPSK 8-state, 2 receive antennas)

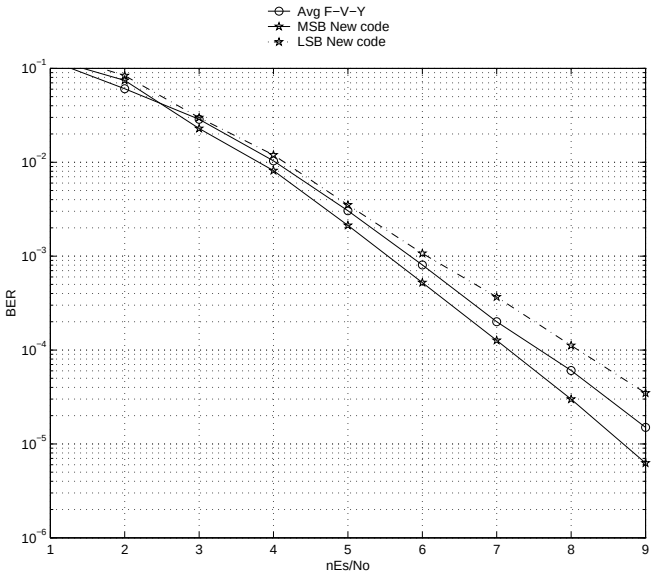

Figure 3.21: Simulation results for the new codes and codes from the literature (QPSK 16-state, 2 receive antennas)

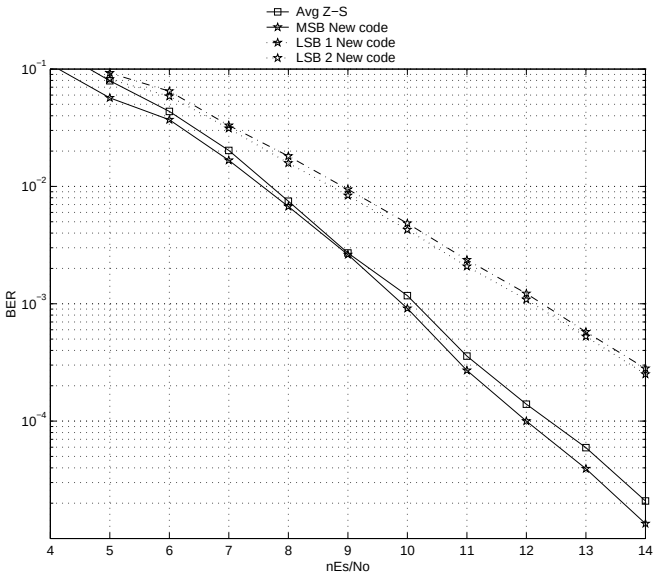

Figure 3.22: Simulation results for the new codes and codes from the literature (8PSK 8-state, 2 receive antennas)

CHAPTER 4

WIRELESS IMAGE TRANSMISSION USING UEP ST TRELLIS CODES

4.1 INTRODUCTION

In the previous chapter, UEP ST-trellis codes have been found and designed. Those codes that offer strong error protection to the most significant bit (MSB) are be applied in this chapter on wireless image transmission. In order to make use of the unequal error protection, the digitized image must first be divided into two or more categories according to importance relative to the human visual system.

This chapter begins by providing the image processing tools needed to categorize the binary stream of bits from the digitized images. The following section contains the application of image transmission.

4.2 IMAGE PROCESSING

Before sending an image using a digital communications system, it must be digitized first. There are many standards and algorithms for image processing. The one to be used here for digitizing images follows that of the popular *JPEG baseline* standard that runs in the *sequential DCT based mode*, defined by the JPEG standard specifications [42]. The encoding process begins by dividing the image into 8×8 blocks on which a forward discrete cosine transformation (FDCT) is computed. The resulting 64 coefficients are quantized and then reordered according to importance. Finally, they are run through a Huffman encoder for lossless compression [42, 43]. In the decoder, the process is reversed. The JPEG image is run through a Huffman decoder, a dequantizer, and an inverse cosine transformer (IDCT).

These steps are used here following the described JPEG baseline standard (will be called JPEG standard for short) except for the lossless compression/decompression part that uses variable length coding. Huffman coding rely on the idea that not all symbols are used with the same probability. Therefore, if symbols that have higher probability of occurance are assigned smaller codewords (codewords with less binary bits representation), then the overall binary bit representation will be smaller. With variable length coding it is necessary to have all bits error-free, in order to correctly decompress them. In this research, SNR is relatively low and hence errors are inevitable. This leads to catastrophic errors with the use of

variable length coding. Instead, a fixed length coding method is used by keeping a fixed number of coefficients from each frame.

4.2.1 Transform Coding

In *transform coding*, a reversible, linear transform is used to map the the image into a set of transform coefficients, which are quantized and coded. For most natural images, a significant number of coefficients have small magnitudes and can be coarsely quantized (or discarded entirely) with little image distortion. The choice of a particular transform in a given application depends on the amount of reconstruction error that can be tolerated and the computational resources available. The lossy compression from transform coding is achieved during the quantization of the transformed coefficients [43].

The optimum transform is the Karhunen-Loéve transform (KLT). It packs the energy into few transform coefficients and the coefficients are as uncorrelated as possible. The drawback of KLT is that it is data-dependent, and is expensive to compute. The discrete cosine transform (DCT) performs very close to KLT especially when the input is a first order Markov process [44]. Because of this reason and that it is relatively cheap to implement, DCT has been used in the JPEG standard.

2-D FDCT is defined as [43]:

$$C(u,v) = \alpha(u) \cdot \alpha(v) \sum_{x=0}^{N-1} \sum_{y=0}^{N-1} f(x,y) \cdot \cos\left(\frac{(2x+1)u\pi}{2N}\right) \cdot \cos\left(\frac{(2y+1)v\pi}{2N}\right) \quad (4.1)$$

where $u,\ v = 0, 1, 2, \ldots, N-1$ and α is given by:

$$\alpha(x) = \begin{cases} \sqrt{\frac{1}{N}} & \text{for } x = 0 \\ \sqrt{\frac{2}{N}} & \text{for } x = 1, 2, \ldots, N-1 \end{cases} \quad (4.2)$$

The 2-D inverse discrete cosine transform (IDCT) is given by:

$$f(x,y) = \sum_{x=0}^{N-1} \sum_{y=0}^{N-1} \alpha(u) \cdot \alpha(v) \cdot C(u,v) \cdot \cos\left(\frac{(2x+1)u\pi}{2N}\right) \cdot \cos\left(\frac{(2y+1)v\pi}{2N}\right) \quad (4.3)$$

for $u,\ v = 0, 1, 2, \ldots, N-1$.

The choice of N (subimages size) is a trade off between quality and computational complexity. The most common subimage size is 8×8 which is the size used in the JPEG standard.

4.2.2 Bit Allocation and Quantization

The most important coefficient, called the DC component (zero frequency coefficient), is the one in the upper left corner of the intensity matrix. It is the average value of the 64 image symbols. The remaining coefficients, called the AC compo-

nents (non-zero frequency coefficients), are not as important as the DC component. Statistically speaking, low frequency components contain more energy than high frequency components [42]. Also, the human perceptual system is more sensitive to low frequency components than high frequency components. After quantization there is a high probability that the values of high frequency coefficients will be zero. This can be viewed that the DCT rearranges image coefficients according to importance. Their importance vary according to their distance from the DC component. Therefore, a zig-zag ordering such as the one in Figure 4.1 is used rearrange coefficients according to importance [43].

Bit allocation commonly denotes the process of quantization and source coding. It follows the computation of the DCT of each block. The bit allocation process makes JPEG a lossy algorithm [42]. There are two main *variable* bit allocation methods: *zonal coding*, and *threshold coding*. In zonal coding, the selection of coefficients to be retained as well as the number of bits used to represent them is chosen on the basis of maximum variance. This requires a priori knowledge of the variance of the DCT coefficients. This procedure can be simplified by basing it on a priori allocation of zero bits to out-of-zone coefficients and a constant number of bits to in-zone coefficients. This latter approach is called *fixed zonal coding*. In threshold coding, the fixed zonal coding approach is made more efficient by basing the in-zone coefficient selection on observed magnitude of coefficients in a particular image rather than a priori. This adaptive procedure prevents the

1	2	6	7	15	16	28	29
3	5	8	14	17	27	30	43
4	9	13	18	26	31	42	44
10	12	19	25	32	41	45	54
11	20	24	33	40	46	53	55
21	23	34	39	47	52	56	61
22	35	38	48	51	57	60	62
36	37	49	50	58	59	63	64

Figure 4.1: Coefficient arrangement matrix

separation of significant frequency components that may lie outside predetermined zones. It is more complex than the fixed zonal coding in the sense that the indexes of chosen coefficients have to be transmitted to the decoder, by means of run-length coding. It is also possible to keep the total number of bits per block constant by using a variable threshold for transmitted coefficient magnitude [45].

In the quantization step each of the 64 DCT coefficients are divided by a user-selectable quantizer step-parameter and rounded to the nearest integer. This is a normalization process. The 64 quantizer step-size parameters form a matrix called the *quantization matrix* (QM). The JPEG standard does not specify the QM. It is up to the user to define the QM (see a typical QM matrix in Figure 4.2). JPEG provides examples of the QM in Annex K of the JPEG standard. The quantization process introduces the distortion that is apparent in the decoded image. The magnitude of the distortion can be varied by changing the quantizer step-size parameters of the QM. This is because an error within the range of one half of the quantizer step-size is introduced during the normalization process. The larger the quantizer step-size, the greater the distortion; the greater the distortion, the smaller the amount of compressed data. This is a typical rate-distortion relationship for lossy compression [42].

Mathematically speaking, each of the 64 DCT coefficients is quantized by a uniform quantizer. For a given quantization matrix with elements Q_{vu} where

16	11	10	16	24	40	51	61
12	12	14	26	26	58	60	55
14	13	16	40	40	57	69	56
14	17	22	51	51	87	80	62
18	22	37	68	68	109	103	77
24	35	55	81	81	104	113	92
49	64	78	103	103	121	120	101
72	92	95	112	112	100	103	99

Figure 4.2: A typical quantization matrix [2]

$u, v = 0, 1, \ldots, 7$, the quantized signal Sq_{vu} is given by the following expression[42]:

$$Sq_{vu} = \left\lfloor \frac{S_{vu}}{Q_{vu}} + 0.5 \right\rfloor \tag{4.4}$$

At the JPEG decoder, this normalization is approximately reversed by dequantization.

$$R_{vu} = Sq_{vu} \times Q_{vu} \tag{4.5}$$

In JPEG baseline, threshold coding followed by Huffman coding is used for sampling and quantization. As pointed out earlier due to the nature of this work, it is necessary to use fixed length coding rather than the variable length coding techniques of variable length coding. Therefore, the bit allocation technique that will be used here is fixed zonal coding bit allocation technique by keeping L coefficients followed by folded binary coding (FBC) [46], [47]. FBC is used since it is more robust to channel errors than natural binary code (NBC) [48]. The reason is that for cases where signal amplitudes near zero are more probable than those away from zero, the FBC would lead to smaller channel error variance than the NBC code [45].

Figures 4.3(a) and 4.3(b) show typical zonal masks [47], [49], [46]. These masks show the number of bits used to encode each of the 64 coefficients. As can be seen, the choice of number of bits changes in accordance with the importance of the coefficient. The DC component is assigned 8 bits, which gives the highest

number of quantization levels among all coefficients. The pattern in which the bits are assigned is consistent with that of zig-zag ordering in accordance with coefficient importance. The zero elements of these matrices are of the discarded DCT coefficients. The matrix of Figure 4.3(a) codes 10 DCT coefficients into 58 bits giving a rate of 0.906 bit per pixel (bpp), while the matrix of Figure 4.3(b) codes 21 DCT coefficients into 96 bits giving a rate of 1.50 bpp. The higher the rate, the less the compression and the better the restored image.

4.2.3 Important vs. Less Important Bits

The new codes proposed in Chapter 3 provide UEP, such that the MSB is given maximum error protection. In order to make use of this property, the image should be divided into two or more categories according to their importance. Even after applying DCT to the image, it is difficult to draw a clear line between what is important and what is less important. Nevertheless, there are two main categories underwhich are four types of bits that can be considered as the most important bits:

- Importance according to DCT coefficients:
  - The DC component in the DCT image.
  - The first few AC components in the DCT image.
- Importance according to bit position in FBC codeword:

8	7	6	4	0	0	0	0
7	6	5	0	0	0	0	0
6	5	0	0	0	0	0	0
4	0	0	0	0	0	0	0
0	0	0	0	0	0	0	0
0	0	0	0	0	0	0	0
0	0	0	0	0	0	0	0
0	0	0	0	0	0	0	0

(a) 10 DCT Coefficients

8	7	6	5	4	2	0	0
7	6	5	4	3	0	0	0
6	5	4	3	0	0	0	0
5	4	3	0	0	0	0	0
4	3	0	0	0	0	0	0
2	0	0	0	0	0	0	0
0	0	0	0	0	0	0	0
0	0	0	0	0	0	0	0

(b) 21 DCT Coefficients

Figure 4.3: Zonal bit allocation matrices

- The sign bit of the FBC codeword.
- The MSB's of the FBC codeword.

The difficulty lies in choosing to include more DCT components, or more bits of every FBC codeword. The solution is somewhere in between. It is important to notice that with the zonal coding technique used here, important DCT components have already an advantage over less important ones. This advantage is in the form of more quantization levels. Therefore, as a general guideline, more emphasis should be on the second category.

In the work of this research, two main types of UEP ST trellis codes have been developed: QPSK and 8PSK. ST trellis QPSK codes take two input bit-streams to the encoder, while 8PSK takes three. This means that the binary image should be divided into two categories of importance for QPSK codes and three categories of importance for 8PSK. In order to split the binary image into multiple streams according to importance, another set of matrices is used. For QPSK codes, the matrices in Figures 4.4(a), 4.4(c), 4.4(b) and 4.4(d) give the two-stream bit allocation for the matrices of Figures 4.3(a) and 4.3(b), respectively. For the MSB (Figures 4.4(a) and 4.4(b)), the numbers in the matrices denote the number of bits that are given higher protection. For example, in the DC component of Figure 4.4(a), 6 bits of the total 8 are considered in the MSB stream. These 6 bits are the sign bit plus the 5 most significant bits of the 8-bit FBC codeword. The remaining 2 bits are considered in the LSB stream, hence the number 2 in the DC

component of the LSB matrix of Figure 4.4(c). For 8PSK codes, there are three streams of bits: one MSB and two LSB as shown in Figures 4.5(a)–4.5(f) for the same 10 and 21 DCT coefficient matrices of Figures 4.3(a) and 4.3(b). The choice of the numbers in the MSB and LSB matrices is ad hoc. Several combinations and choices have been tested until these numbers were settled upon. Nevertheless, the choice makes sense, since it follows the guidelines presented above. It can be seen that in the MSB matrices, more bits are included from the DC component and the more important AC components.

The sign bits of the DC component and the first two AC components can be labeled as the most important among the MSB. Additional protection can be applied to these exceptionally important bits to increase image transmission quality. One way to increase protection is use concatenation coding in the form of a Hamming code concatenated by the ST trellis code. The increase of the bit rate due to the additional redundancy may not be desirable. Therefore, the number of FBC bits assigned to less important AC coefficients can be decreased to be replaced by the additional coded bits. The downside is that decreasing the number of bits decreases the number of quantization levels, which in turn, increases quantization noise. Nevertheless, the coding gain should compensate for that loss and increase the overall quality of image transmission for relatively low SNR.

6	4	3	1	0	0	0	0
4	3	2	0	0	0	0	0
3	2	0	0	0	0	0	0
1	0	0	0	0	0	0	0
0	0	0	0	0	0	0	0
0	0	0	0	0	0	0	0
0	0	0	0	0	0	0	0
0	0	0	0	0	0	0	0

(a) 10 DCT - MSB

5	5	3	2	2	1	0	0
5	3	2	2	1	0	0	0
3	2	2	1	0	0	0	0
2	2	1	0	0	0	0	0
2	1	0	0	0	0	0	0
1	0	0	0	0	0	0	0
0	0	0	0	0	0	0	0
0	0	0	0	0	0	0	0

(b) 21 DCT - MSB

2	3	3	3	0	0	0	0
3	3	3	0	0	0	0	0
3	3	0	0	0	0	0	0
3	0	0	0	0	0	0	0
0	0	0	0	0	0	0	0
0	0	0	0	0	0	0	0
0	0	0	0	0	0	0	0
0	0	0	0	0	0	0	0

(c) 10 DCT - LSB

3	2	3	3	2	1	0	0
2	3	3	2	2	0	0	0
3	3	2	2	0	0	0	0
3	2	2	0	0	0	0	0
2	2	0	0	0	0	0	0
1	0	0	0	0	0	0	0
0	0	0	0	0	0	0	0
0	0	0	0	0	0	0	0

(d) 21 DCT - LSB

Figure 4.4: QPSK MSB and LSB bit allocation matrices

5	2	2	1	0	0	0	0
2	2	1	0	0	0	0	0
2	1	0	0	0	0	0	0
1	0	0	0	0	0	0	0
0	0	0	0	0	0	0	0
0	0	0	0	0	0	0	0
0	0	0	0	0	0	0	0
0	0	0	0	0	0	0	0

(a) 10 DCT - MSB

5	3	2	1	1	1	0	0
3	2	1	1	1	0	0	0
2	1	1	1	0	0	0	0
1	1	1	0	0	0	0	0
1	1	0	0	0	0	0	0
1	0	0	0	0	0	0	0
0	0	0	0	0	0	0	0
0	0	0	0	0	0	0	0

(b) 21 DCT - MSB

2	3	2	1	0	0	0	0
3	2	1	0	0	0	0	0
2	2	0	0	0	0	0	0
1	0	0	0	0	0	0	0
0	0	0	0	0	0	0	0
0	0	0	0	0	0	0	0
0	0	0	0	0	0	0	0
0	0	0	0	0	0	0	0

(c) 10 DCT - LSB 1

2	3	2	1	1	1	0	0
3	2	2	1	1	0	0	0
2	3	1	1	0	0	0	0
2	1	1	0	0	0	0	0
1	1	0	0	0	0	0	0
1	0	0	0	0	0	0	0
0	0	0	0	0	0	0	0
0	0	0	0	0	0	0	0

(d) 21 DCT - LSB 1

1	2	2	2	0	0	0	0
2	2	2	0	0	0	0	0
2	2	0	0	0	0	0	0
2	0	0	0	0	0	0	0
0	0	0	0	0	0	0	0
0	0	0	0	0	0	0	0
0	0	0	0	0	0	0	0
0	0	0	0	0	0	0	0

(e) 10 DCT - LSB 2

1	1	2	3	1	1	0	0
1	2	2	2	1	0	0	0
2	2	2	1	0	0	0	0
2	2	1	0	0	0	0	0
1	1	0	0	0	0	0	0
1	0	0	0	0	0	0	0
0	0	0	0	0	0	0	0
0	0	0	0	0	0	0	0

(f) 21 DCT - LSB 2

Figure 4.5: 8PSK MSB, LSB 1, and LSB 2 bit allocation matrices

4.3 Image Transmission Over a Rapid Fading Channel Using ST-Trellis Coding

In this section, the application of image transmission over a rapid fading channel is examined. Several codes over various signal-to-noise ratios are tested. The goal is to test the ability of unequal error protecting codes (UEP) of providing better image quality at the same SNR compared to equal error protecting codes (EEP) found in the literature. To provide a quantitative measurement of image quality, one can reside to several quality indexes. One widely used image quality measurement index is the peak signal-to-noise ratio (PSNR) index. For an $N \times M$ 256-levels, grayscale image, PSNR is given by [44]:

$$\text{PSNR} = 10 \log_{10} \left(\frac{255^2}{\frac{1}{NM} \sum_{n=1}^{N} \sum_{m=1}^{M} (x(n,m) - \hat{x}(n,m))^2} \right) \tag{4.6}$$

where $x(n,m)$ and $\hat{x}(n,m)$ denote the original and transmitted images' intensity at pixel (n,m), respectively.

The method used in image processing is the same as the one described in section 4.2. The image of choice is the *Cameraman* image of size 256×256 pixels. The image is divided into 8×8 blocks. After the DCT is computed, each block is normalized, quantized and coded using FBC, following the method of fixed Zonal coding. In order to use different compression values, two bit rates are used. For

this purpose the bit allocation matrices used are those of 4.3(a) and 4.3(b) that keep 10 and 21 DCT coefficients and provide bit rates of 0.906 and 1.50 bpp, respectively.

4.3.1 QPSK Codes

The new codes, from both design and search approaches, have identical performance (see Section 3.5). Therefore, only designed codes from Figure 3.8 are going to be considered here for simulation. In order to compare their simulation performance to other known good codes in the literature, the codes of Fermanto *et al* [12] are considered (referred to as F-V-Y codes).

The MSB and LSB matrices used are those of 4.2.3. For the added protection a (7, 4) single error correcting Hamming code is used to encode 4 of the exceptionally important MSB into 7 encoded bits. This code will be referred to as the *new code with Hamming* to distinguish between it and the new code *without* Hamming encoding that will be referred to simply as the *new code*. The addition of the 3 bits will be balanced by terminating 3 bits from the LSB.

The first code to be tested is the 4-state code from Figure 3.8. The cameraman image have been simulated for transmission over a rapid fading channel with relatively low signal-to-noise ratios. Moreover, this same code with the concatenation of a (7, 4) Hamming is simulated over the same channel. For comparison Fermanto 4-state code is also simulated over this channel. The PSNR of sending

cameraman with 10- and 21-DCT coefficients is shown in Figures 4.6(a) and 4.6(b), respectively. From these plots, the following results can be noticed:

- 21-DCT coefficients codes perform better than 10-DCT coefficients codes, which is expected since the rate is higher.
- Gains of 0.5 to 1.5 dB are achieved for the new code with Hamming SNR less than 8 dB.
- Gains of 0.25 to 1.25 dB are achieved for the new code for SNR less than 8 dB.
- All three codes have almost identical performance for SNR higher than 8 dB.
- At High SNR, the new code with Hamming has lower PSNR, because of the truncation of the 3 LSB's.

These results can be noticed in the restored images shown in Figures 4.7 and 4.8 for 10 and 21 DCT coefficients, respectively. At 5 dB, the new code is better than F-V-Y, and the new code with Hamming is the best among them (See Figures 4.7(a), 4.7(c) and 4.7(e), respectively). A similar result can be seen for SNR = 8 dB. The 21-DCT coefficients (Figure 4.8) perform better than 10-DCT coefficients, as was concluded from the PSNR plots. Again, the restored image's quality increases in the new code from F-V-Y code and in the new code with Hamming from the new code.

Increasing the number of states, enhances the code's performance on the expense of increasing the code's complexity. Nevertheless, the same results that were presented above for 4-state QPSK codes, apply for 8 and 16-state QPSK codes, as can be seen from PSNR plots of Figures 4.9 and 4.12 for both 10 and 21-DCT coefficients. Similarly, the image quality is slightly better in the new code and is the best in the new code with Hamming (see Figures 4.10, 4.11, 4.13, and 4.14). The difference is that the dB gain at the same PSNR is less for 8 and 16-state compared to 4-state. The gain in 8 and 16-state codes is around 1.0 and 0.5 dB, respectively between the new code with Hamming and F-V-Y code. Between the new code and F-V-Y code the gain is around 0.5 and 0.25 for 8 and 16-state codes, respectively. This small gain from the PSNR plot is minorly evident in the restored images. In fact, there are almost no visual differences between various coding techniques in the 16-state case.

4.3.2 8PSK Codes

8PSK codes have three input bits to the encoder. Therefore, the rate is higher, but the average power is the same. This results in a performance that is inferior to QPSK codes. As mentioned earlier in Section 4.2 for 8PSK, the zonal bit allocation matrices are divided into three matrices: one being the MSB matrix and the other two are LSB. The MSB and LSB matrices used are those of 4.2.3. For added protection a (7, 4) single error correcting Hamming code is used to encode 4 of the

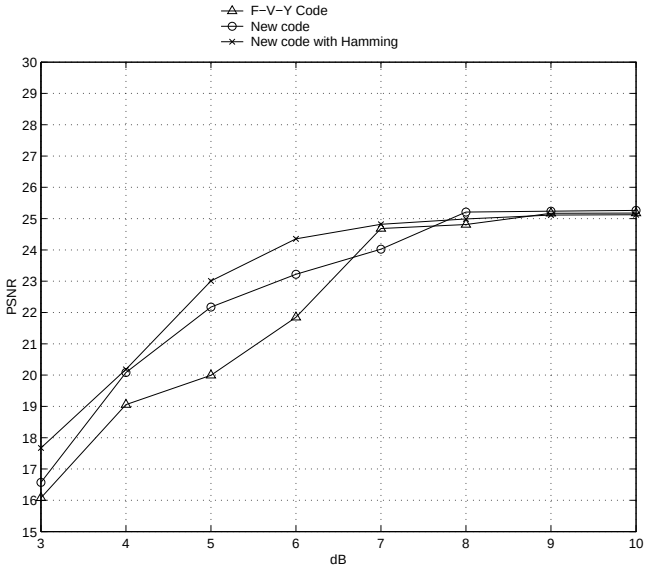

(a) 10 DCT coefficients

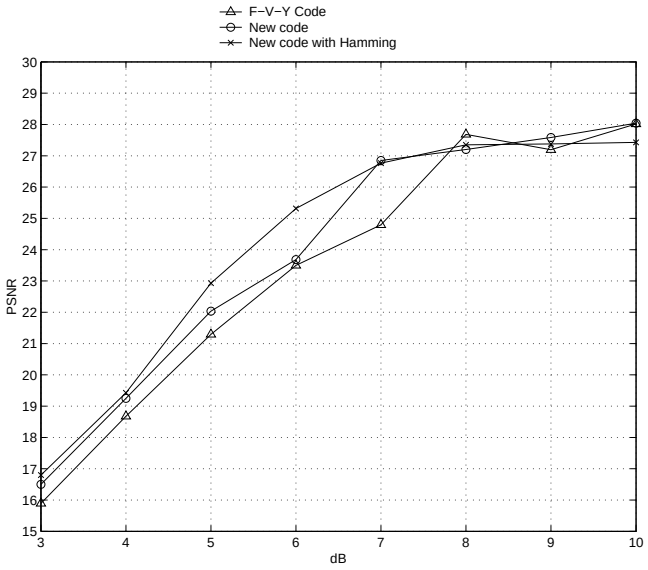

(b) 21 DCT coefficients

Figure 4.6: QPSK 4-state PSNR

(a) F-V-Y, 5 dB

(b) F-V-Y, 8 dB

(c) New code, 5 dB

(d) New code, 8 dB

(e) New code with Hamming, 5 dB

(f) New code with Hamming, 8 dB

Figure 4.7: 4-state QPSK codes, 10 DCT Coefficients

(a) F-V-Y, 5 dB

(b) F-V-Y, 8 dB

(c) New code, 5 dB

(d) New code, 8 dB

(e) New code with Hamming, 5 dB

(f) New code with Hamming, 8 dB

Figure 4.8: 4-state QPSK codes, 21 DCT Coefficients

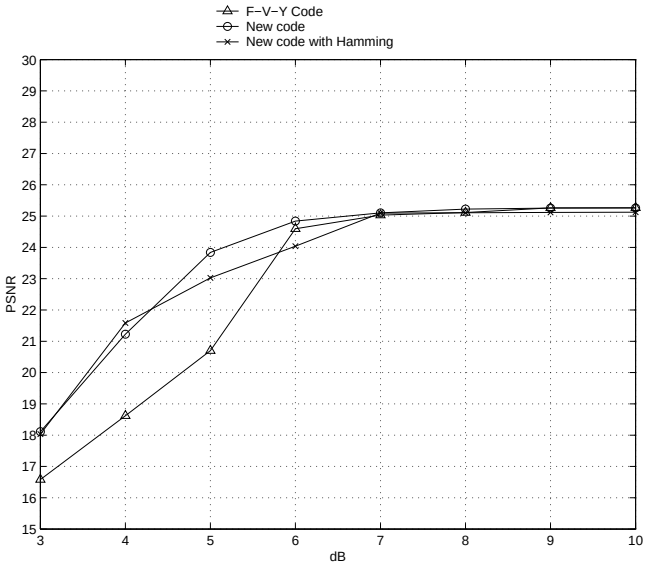

(a) 10 DCT coefficients

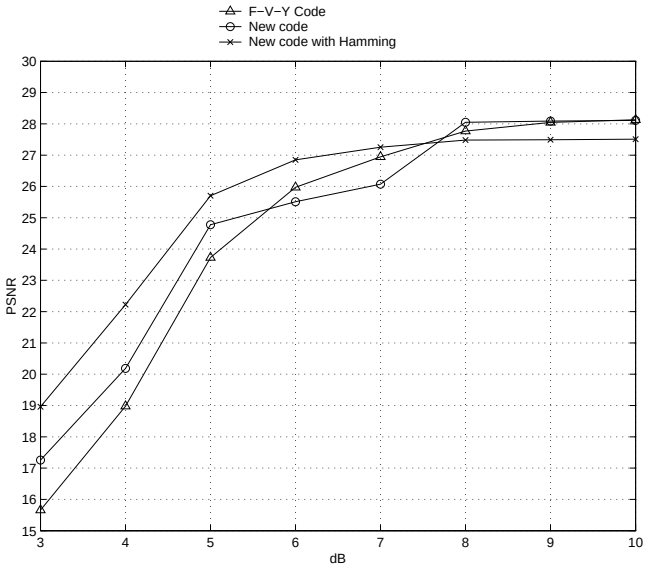

(b) 21 DCT coefficients

Figure 4.9: QPSK 8-state PSNR

(a) F-V-Y, 5 dB

(b) F-V-Y, 8 dB

(c) New code, 5 dB

(d) New code, 8 dB

(e) New code with Hamming, 5 dB

(f) New code with Hamming, 8 dB

Figure 4.10: 8-state QPSK codes, 10 DCT Coefficients

(a) F-V-Y, 5 dB

(b) F-V-Y, 8 dB

(c) New code, 5 dB

(d) New code, 8 dB

(e) New code with Hamming, 5 dB

(f) New code with Hamming, 8 dB

Figure 4.11: 8-state QPSK codes, 21 DCT Coefficients

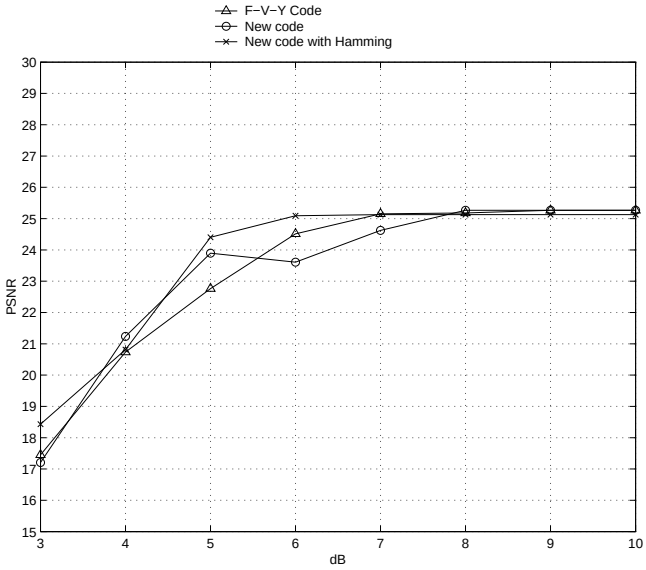

(a) 10 DCT coefficients

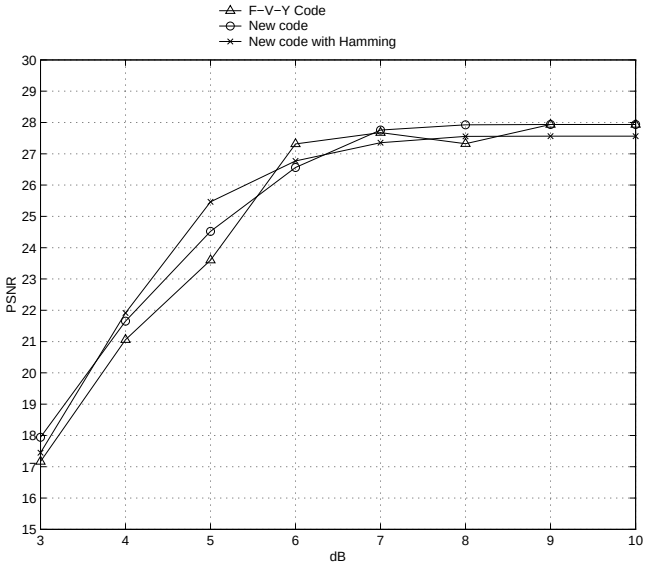

(b) 21 DCT coefficients

Figure 4.12: QPSK 16-state PSNR

(a) F-V-Y, 5 dB

(b) F-V-Y, 8 dB

(c) New code, 5 dB

(d) New code, 8 dB

(e) New code with Hamming, 5 dB

(f) New code with Hamming, 8 dB

Figure 4.13: 16-state QPSK codes, 10 DCT Coefficients

(a) F-V-Y, 5 dB

(b) F-V-Y, 8 dB

(c) New code, 5 dB

(d) New code, 8 dB

(e) New code with Hamming, 5 dB

(f) New code with Hamming, 8 dB

Figure 4.14: 16-state QPSK codes, 21 DCT Coefficients

exceptionally important MSB into 7 encoded bits. The addition of the 3 bits will balanced by terminating 3 bits from the LSB. Again, the codes from both design and search approaches are identical (see Section 3.5), and only the designed code will be considered here. In the 8PSK case the comparison code is the one proposed by Zummo and Al-Semari in [40] and called QPSK3 (referred to as Z-S code).

The three codes, namely Z-S code, the new code and the new code with Hamming, are used to send the same cameraman image over a rapid fading channel using the same technique described earlier for QPSK. This is done twice: first for 10-DCT coefficients and second for 21-DCT coefficients. PSNR plot for both cases is in Figure 4.15. The results are similar to the ones reported for QPSK, but with some differences:

- 21-DCT coefficients codes perform better than 10-DCT coefficients codes.
- Gains of 0.25 to 1.0 dB are achieved for the new code with Hamming SNR less than 10 dB.
- Gains of 0.25 to 0.75 dB are achieved for the new code for SNR less than 10 dB.
- All three codes have almost identical performance for SNR higher than 10 dB.
- At High SNR, the new code with Hamming has lower PSNR, because of the truncation of the 3 LSB.

These results can be noticed in the restored images shown in Figures 4.16 and 4.17 for 10 and 21 DCT coefficients, respectively. At 8 dB, the new code is better than Z-S code, and the new code with Hamming is the best among them (See Figures 4.16(a), 4.16(c) and 4.16(e), respectively). A similar result can be seen for SNR = 10 dB. The 21-DCT coefficients (Figure 4.17) perform better than 10-DCT coefficients, as was concluded from the PSNR plots. Again, the restored image's quality increases in the new code from Z-S code and in the new code with Hamming from the new code.

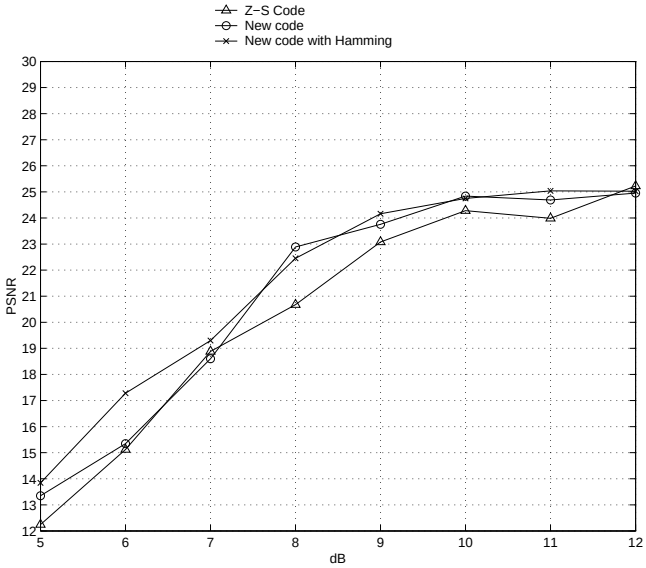

(a) 10 DCT coefficients

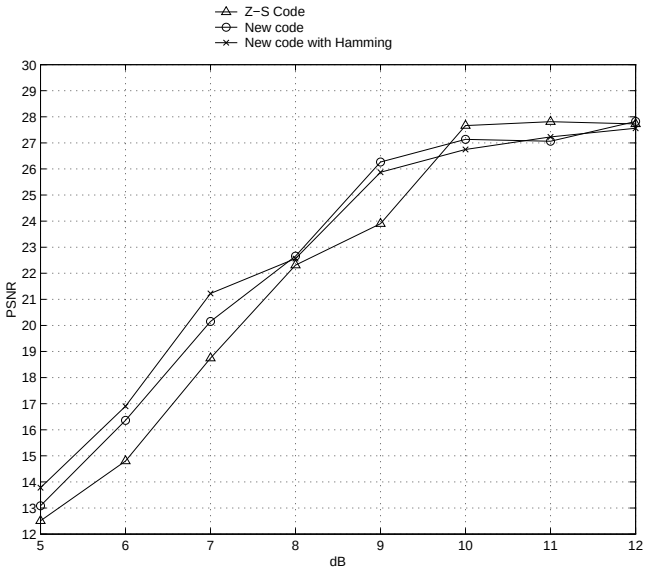

(b) 21 DCT coefficients

Figure 4.15: 8PSK 8-state PSNR

(a) Z-S, 7 dB

(b) Z-S, 10 dB

(c) New code, 7 dB

(d) New code, 10 dB

(e) New code with Hamming, 7 dB

(f) New code with Hamming, 10 dB

Figure 4.16: 8PSK codes, 10 DCT Coefficients

(a) Z-S, 7 dB

(b) Z-S, 10 dB

(c) New code, 7 dB

(d) New code, 10 dB

(e) New code with Hamming, 7 dB

(f) New code with Hamming, 10 dB

Figure 4.17: 8PSK codes, 21 DCT Coefficients

CHAPTER 5

CONCLUSIONS AND FUTURE RESEARCH

5.1 SUMMARY AND CONCLUSIONS

In this thesis, the performance of ST trellis codes over rapid fading channels have been studied. A wireless transmitter/receiver system has been simulated using C programming and tested over quasi-static and rapid fading channels using various codes from the literature.

It has been shown and proven that certain ST trellis codes provide unequal error-protection to different input. In order to show the weight of error protection on individual input bits, the transfer function, as a performance evaluation technique has been reviewed in Chapter 2. Then, a modified version of the transfer

function that shows the weight of error protection on every input bit has been derived. From the modified transfer function, new BEP upper-bounds have been derived for individual input bits. The modified distance spectrum has been used as a method to enumerate the modified transfer function. Expanding the transfer to find the distance spectrum of general trellis codes is a complicated task. It can be simplified if the code is quasi-regular. In this thesis, the definition of quasi-regularity is extended to ST trellis codes. Furthermore, several examples of quasi-regular, non-quasi-regular, distance spectrum and upper-bounds for individual input bits are provided in this chapter.

Two approaches were used to find ST trellis codes that provide very strong error protection to the most significant bit. Before describing the approaches, general guidelines efficient design and search criteria were developed from the modified performance evaluation techniques. The first approach is an exhaustive search approach which is performed in two steps. First, all possible codes of a certain modulation scheme and a certain number of states are generated assuming a linear encoder. Then all generated codes are passed through a series of tests to find the best ones satisfying the search criteria. To speed up this lengthy process, the programming was done in C language. The second approach is a design approach, in which a new 7-step design technique is introduced. Although, there are good design approaches in the literature, but none of them consider the weight of error protection on different input bits. This new design technique considers the task

of addressing input bits individually, in terms of error protection weight. Hence, it is capable of handcrafting codes that provide unequal error protection. Both approaches have been used to find 4, 8 and 16-state QPSK and 8-state 8PSK codes providing strong error protection properties to the most significant bit. The new codes have better minimum product distance properties for the MSB. Simulation showed that the improvement is relatively low at low SNR values, but the gain increases at high SNR. The largest gain was for the 8-state QPSK code, which gave a gain of more than 1.5 dB over the nearest code from the literature at a bit error rate BER = 10^{-5}. On the other hand, the smallest gain was for the 8-state 8PSK code, which was around 0.5 dB at BER = 10^{-5}. In the cases of 4 and 16-state QPSK, the gain was around 1.0 and 0.75 dB at BER = 10^{-5}, respectively.

In order to complete the application of image transmission, the image was processed such that it followed, as much as possible, the popular JPEG standard. The image was transformed then quantized. Instead of using variable length coding in the last step of image processing, a modified approach that uses fixed length zonal coding has been adopted to avoid propagation of error problem. This approach reduces the number of bits to represent coefficients (similar to variable length coding) using the fact that the DCT coefficients do not have the same maximum variance. In order to make use of the added protection to the MSB in the new codes, the digitized image has been divided into more than one bit stream according to importance. The bit division technique has been chosen such that the MSB

category includes the most important bits of every coefficient and more bits from the most important coefficients. This hybrid technique proved to be effective in the application.

The new codes, along with several codes from the literature, were used to simulate the transmission of a test image that was processed in the proposed technique over a rapid fading channel. PSNR plots showed gains of 0.25 to 1.25 dB at low SNR for the new codes over the codes from the literature. An additional 0.5 dB improvement was reached using a concatenation of a simple (7, 4) Hamming code. These improvements were evident to the human eye on the retrieved images. The new codes and image processing technique provided an enhanced image quality for relatively low SNR wireless transmission using the new codes compared to other codes in the literature.

5.2 Future Work

- The design and search of new codes can be extended to higher constellations such as 16, 32 and 64-QAM in the same manner used in this research. Going to to different constellations may provide more ways to enhance error protection on the MSB.

- A different approach of unequal error protection that uses unequal power assignment to input bits can be used. Non-uniformly spaced constellation

points are used and the MSB is assigned to the constellation points with higher power. This approach that was used for conventional trellis coding in [50] needs higher constellations than the ones used in this research.

- Another approach of unequal error protection is code concatenation. The most important bits can be provided the additional protection using code concatenation. A possible code concatenation techniques that can be used for the image transmission application is concatenating Reed-Solomon with ST trellis codes.

- Other image standards, such as vector quantization and JPEG 2000, can be applied to provide possible enhancement. The enhancement can happen because of the possible different ways of image division according to importance.

- The new unequal error protecting codes found in this work can be applied to other applications, such wireless voice communication. Voice communication is similar to image communication in the sense that it is tolerant to data errors. The voice can be divided into multiple streams of bits according to importance and sent using the new codes to provide strong error protection to the MSB.

- The code search approach can be applied to more complicated codes such as 32 and 64-state QPSK and 16 and 32-8PSK codes. The problem is that

the search scope can get so huge that exhaustive search is no longer feasible. Genetic algorithms, or any other non-exhaustive search approach can be used to do such a task.

- The work in this thesis is limited to rapid fading channels, but can be extended to quasi-static channels. The whole approach would need to be modified since the distance and product criteria are not the performance merits. Designing unequal error protecting codes for quasi-static channels in a similar approach to the one used in this thesis would require using a different symmetry property other than quasi-regularity for path enumeration. Also, the design steps and the search criteria will need to be changed totally.

- A new family of unequal error protecting codes can be proposed based on the approaches used in this work. Instead of providing the best possible error protection to the MSB, a new family of codes that provides different error protection degrees to the input bits can be used. The code is chosen depending on the application requirement of maximum protection to the MSB, equal protection to both bits, or somewhere in between.

BIBLIOGRAPHY

[1] Vahid Tarokh, Nambi Seshadri, and A. R. Calderbank. Space-time codes for high data rate wireless communication: Performance criterion and code construction. *IEEE Transactions on Information Theory*, 44(2):744–765, Mar 1998.

[2] William B. Pennebaker and Joan L. Mitchell. *JPEG: Still Image Data Compression Standard*. Van Nostrand Reinhold, 1993.

[3] John G. Proakis. *Digital Communications*. McGraw-Hill, fourth edition, 2001.

[4] Simon Haykin. *Communication Systems*. John Wiley & Sons, Inc., third edition, 1994.

[5] W. Kuo and M. Fitz. Design and analysis of transmitter diversity using intentional frequency offset for wireless communication. *IEEE Trans. on Veh. Tech.*, Nov 1997.

[6] S. H. Jamali and T. Le-Ngoc. *Coded-Modulation Techniques for Fading Channels*. Massachsetts: Kluwer Academic Publisher, 1994.

[7] Ezio Biglieri, Dariush Divsalar, Peter J. McLane, and Marvin K. Simon. *Introduction to Trellis-Coded Modulation with Applications*. Macmillan Publishing Company, 1991.

[8] A. Wittneben. Base station modulation diversity in wireless systems with Rayleigh fading. *Proc. IEEE Veh. Tech.*, pages 505–511, May 1993.

[9] Stephen Bäro, Gerhard Bauch, and Axel Hansmann. Improved codes for space-time trellis-coded modulation. *IEEE Communication Letters*, 4(1):20–22, Jan 2000.

[10] Salam A. Zummo and Saud A. Al-Semari. Space-time coded QPSK for rapid fading channels. *PIMRC*, 1(1):504–508, Sep 2000.

[11] Qing Yan and Rick S. Blum. Optimum space-time convolutional codes. *Wireless Communications and Networking Conference*, 3:1351–1355, Sep 2000.

[12] Welly Firmanto, Branka S. Vucetic, and Jinhong Yuan. Space-time TCM with improved performance on fast fading channels. *IEEE Communication Letters*, 5(4):154–156, Apr 2001.

[13] George Azevedo da Selva. Some new codes for space-time trellis encoded modulation over fading ISI channels. *PIMRC*, Sep 2000.

[14] J. Grimm and M. P. Fitz. Further results on space-time coding for Rayleigh fading. *Proc. of the 1998 Allerton Conf.*, pages 391–400, Sep 1998.

[15] Rick S. Blum. Analytical tools for the design of space-time convolutional codes. *Conference on Information Sciences and Systems*, Mar 2000.

[16] Krishna Kiran Mukavilli, D. Mihai Ionescu, and Bechnaam Aazhang. Design of space-time codes with optimal coding gain. *PIMRC*, Sep 2000.

[17] Jr. A. Roger Hammons and Hesham El Gamal. On the theory of space-time codes for PSK modulation. *IEEE Transactions on Information Theory*, 46(2):524–542, Mar 2000.

[18] Youjian Liu, Michael P. Fitz, and Oscar Y. Takeshita. A rank criterion for QAM space-time codes. *First IEEE Sensor Array and Multichannel Signal Processing Workshop*, Mar 2000.

[19] Siwaruk Siwamogsatham and M. Fitz. Robust space-time coding for correlated Rayleigh fading channels. *Proc. 38th Annual Allerton Conf. on Communication, Control, and Computing*, Oct 2000.

[20] Youjian Liu, Michael P. Fitz, and Oscar Y. Takeshita. QPSK space-time turbo codes. *International Conference on Communications*, Jun 2000.

[21] Xiaotong Lin and Rick S. Blum. Imporved space-time codes using serial concatenation. *IEEE Communication Letters*, pages 221–223, Jul 2000.

[22] Xiaotong Lin and Rick S. Blum. On the design of space-time codes employing multiple trellis coded modulation. *Conference on Information Sciences and Systems*, Mar 2000.

[23] Michael P. Fitz and Jimm Grimm. A new view of performance analysis techniques in correlated Rayleigh fading. *Wireless Communications and Networking Conference*, 1:139–144, Sep 1999.

[24] Markku J. Heikkila, Kari Majonen, and Jorma Lilleberg. Decoding and performance of space-time trellis codes in fading channels with intersymbol interference. *Proceedings of the 11th IEEE International Symposium on Personal, Indoor and Mobile Radio Communications (PIMRC)*, 1(1):490–494, Sep 2000.

[25] Salam A. Zummo and Saud A. Al-Semari. A tight bound on the error probability of space-time codes for rapid fading channels. *Wireless Communications and Networking Conference*, 3:23–28, Sep 2000.

[26] Define K. Aktas and Michael P. Fitz. Computing the distance spectrum of space-time trellis codes. *Wireless Communications and Networking Conference*, Sep 2000.

[27] Define K. Aktas and Michael P. Fitz. Distance spectra of space-time trellis coded modulations. *IEEE International Symposium on Information Theory*, June 2001.

[28] Xiaoxia Zhang and Michael Fitz. Space-time coding for Rayleigh fading channels in CPM system. *Proc. 38th Annual Allerton Conf. on Communication, Control, and Computing*, Oct 2000.

[29] Abdelgader M. Legnain and David D. Falconer. Transient behavior of the linear adaptive combined space-time receiver for DS-CDMA systems. *PIMRC*, Sep 2000.

[30] Yumin Zhang and Rick S. Blum. Multistage multiuser detection for CDMA with space-time coding. *IEEE Workshop on Statistical Signal and Array Processing (SSAP2000)*, Aug 2000.

[31] E. Biglieri. High-level modulation and coding for nonlinear satelite channels. *IEEE Transactions on Communications*, 32:616–626, May 1984.

[32] M. Rouanne and Jr D. J. Costello. An algorithm for computing the distance spectrum of trellis codes. *IEEE Journal on Selected Areas in Communications*, 7(6):929–940, Aug 1989.

[33] E. Zehavi and J. K. Wolf. On the performance evaluation of trellis codes. *IEEE Transactions on Communications*, 33(2):196–202, Mar 1987.

[34] A. R. Calderbank and N. J. Sloane. New trellis codes based on lattices and subsets. *IEEE Transactions on Information Theory*, 33(2):177–195, Mar 1987.

[35] Richard D. Wesel. Reduced complexity trellis code transfer function computation. *Communication Theory Mini-Conference*, pages 37–41, June 1999.

[36] G. D. Forney. Geometrically uniform codes. *IEEE Transactions on Information Theory*, 37(5):1241–1260, Sep 1991.

[37] S. Benedetto, M. Mondin, and G. Montorsi. Performance evaluation of trellis-coded modulation schemes. *Proceedings of the IEEE*, 82(6):833–855, Jun 1994.

[38] D. G. Mills and D. J. Costello. Using a modified transfer function to calculate unequal error protection capabilities of convolutional codes. *IEEE Proceedings on Information Theory*, page 144, 1993.

[39] J. K. Omura and M. K. Simon. Generalized transfer function techniques. *Jet Propultion Laboratories Technical Report*, 1981.

[40] Salam A. Zummo and Saud A. Al-Semari. Space-time trellis coded 8-PSK schemes for rapid fading Rayleigh channels. *EURASIP Journal on Applied Signal Processing*, 5:482–486, May 2002.

[41] Elvio J. Leonardo, Lin Zhang, and Branka S. Vucetic. Multidimensional M-PSK trellis codes for fading channels. *IEEE Transactions on Information Theory*, 42(4):1093–1108, Jul 1996.

[42] Weidong Kou. *Digital Image Compression: Algorithms and Standards*. Kluwer Academic Publishers, 1995.

[43] Rafael C. Gonzalez and Richard E. Woods. *Digital Image Processing*. Addison-Wesley Publishing Company, Inc., Sep 1993.

[44] Vijay K. Madisetti and Douglas B. Williams*, editors*. *The Digital Signal Processing Handbook*. CRC Press and IEEE Press, 1998.

[45] N. S. Jayant and Peter Noll. *Digital Coding of Waveforms*. Prentice-Hall, Inc., 1984.

[46] A. M. Tekalp. *Digital Video Processing*. Prentice-Hall, Inc., 1995.

[47] Fady I. Alajaji, Saud A. Al-Semari, and Philppe Burlina. Visual communication via trellis coding and transmission energy allocation. *IEEE Transactions on Communications*, 47(11):1722–1728, Nov 1999.

[48] Wen Xu, Joachim Hagenauer, and Jürgen Hollmann. Joint source-channel decoding using the resident redundancy in compressed images. *Proceedings of International Conference in Communications*, Jun 1996.

[49] Philppe Burlina and Fady I. Alajaji. An error resilient scheme for image transmission over noisy channels with memory. *IEEE Transactions on Image Processing*, 7(4):593–600, Apr 1998.

[50] Lee-Fang Wei. Coded modulation with unequal error protection. *IEEE Transactions on Communications*, 41(10):1439–1449, Oct 1993.

[51] Bernard Sklar. *Digital Communications*. Prentice-Hall, first edition, 1988.

[52] Al Bovik, *editor. Handbook of Image and Video Processing.* Academic Press, 2000.

[53] Ezio Biglieri, Dariush Divsalar, Peter J. McLane, and Marvin K. Simon. *Introduction to Trellis-Coded Modulation with Applications.* Macmillan Publishing Company, 1991.

[54] Salam Adel Zummo. Performance and design of space-time trellis codes for wireless channels. Master's thesis, KFUPM, Dec 1999.

[55] Tai-Ann Chen, Michael P. Fitz, Wen-Yi Kuo, Michael D. Zoltowski, and Jimm H. Grimm. A space-time model for frequency nonselective Rayleigh fading channels with applications to space-time modems. *IEEE Journal on Select Areas in Communications*, 18(7):1175–1190, Jul 2000.

[56] Salam A. Zummo and Saud A. Al-Semari. Improved space-time QPSK codes for rapid fading channels. *IEEE Vehicular Technology Conference*, 2000.

[57] S. Benedetto, M. A. Marsan, G. Albertengo, and E. Giachin. Combined coding and modulation: Theory and applications. *IEEE Transactions on Information Theory*, 34(2):223–236, Mar 1988.

[58] Saud A. Al-Semari and Thomas E. Fuja. Performance analysis of coherent tcm systems with diversity reception in slow rayleigh fading. *IEEE Transactions on Vehicular Technology*, 48(1):198–212, Jan 1999.

VITA

- Hesham Muhammad Ibrahim al-Salman.
- Born in Jalajil, Saudi Arabia on July 17, 1977.
- Received Bachelor of Engineering (B.E) degree with Highest Honors in Electrical Engineering from King Fahd University of Petroleum and Minerals, Dhahran, Saudi Arabia in December 1999.
- Email: alsalman@kfupm.edu.sa